Energy Reports 15 (2026) 109146

Contents lists available at ScienceDirect

Energy Reports

journal homepage: www.elsevier.com/locate/egyr

Research paper

Optimization-based integration of a metal hydride storage in a residential energy system – A techno-economic analysis

Chris Drawer *, Luka Bornemann, Martin Kaltschmitt

Institute of Environmental Technology and Energy Economics (IUE), Hamburg University of Technology (TUHH), Eissendorfer Strasse 40, Hamburg 21073, Germany

ARTICLE INFO

Keywords:
Metal hydride storage
Energy system optimization
Residential energy system
Autarky

ABSTRACT

The increased use of electrified heating systems in residential buildings places additional demands on the power grid, alongside the growing load from, e.g., photovoltaic power. One solution to relieve the strain on the power grid could be to increase the energy autarky of residential buildings by increasing the consumption of self-generated electricity. Higher self-consumption requires an energy storage system that is capable of storing large amounts of electricity (seasonally). Metal hydride storage systems could be a technically feasible solution. Excess heat from the metal hydride storage tank could contribute to the heating system and further reduce electricity consumption. This study aims to investigate the extent to which a metal hydride storage system can be used in a single-family house to relieve stress on the power grid significantly. To investigate this novel approach, a design and operation optimization is performed to determine the most cost-effective system configuration at maximum autarky level. Compared to a reference case with no seasonal energy storage, the autarky level could be increased by integrating a metal hydride storage system by 27%-points to 79% resulting in a feed-in reduction of 35% into the superior power grid. In addition, grid electricity consumption can be reduced by up to 45%. However, such a system results in a 4.3-fold increase in total annual costs. Even with positive developments in the future (technological and economic), this factor can only be reduced to 2.5. Independent of the clear cost increase under current cost relations, the integration of metal hydride storage systems into a future home energy system is a technically viable option.

1. Introduction

In order to reduce greenhouse gas emissions, one of the most important measures is to switch the energy supply from fossil fuels to renewable energy sources. This is true on a large scale (e.g., offshore wind parks in the North Sea) as well as on a small scale; the latter includes, in particular, the residential sector. Here, a rapid increase in the expansion of photovoltaic (PV) systems on house roofs, especially on single-family houses, can be observed, e.g., in Europe (Observ'ER et al., 2024). In addition, there is a shift away from oil and gas for heating, particularly in new buildings, towards heat pump systems powered by electricity (Olympios et al., 2025).

This increasing number of decentralized house energy systems in Europe, which, unlike conventional energy systems implemented so far, not only draw electricity but can also feed it into the superior public grid, represents a strongly growing local burden on the power grid in addition to the rising demand for electricity (Spalthoff et al., 2022). Furthermore, electricity from PV systems is typically not available on demand, but is produced in excess during the day when demand is low (mainly during the summer), while in the late evening or early morning (and especially during the night), limited or no PV electricity is available. This results in the fact that, on average, only 20 – 50% of the electricity demand of such small-scale residential energy systems can be covered by PV systems (Wirth and Fraunhofer ISE, 2025).

One solution that can both relieve the load on the electricity grid and increase self-use of PV electricity, thereby increasing independence from the public electricity grid, is seasonal storage of self-produced PV electricity. Today, when combined with PV systems, battery storage systems often lead to increased use of self-generated electricity; however, these systems are clearly limited to storing electricity in the medium- to long-term (Durán Gómez et al., 2023). But long-term or seasonal storage is essential to improve the autarky of single-family houses and reduce strain on the power grid. Thus, this study focuses on seasonal energy storage for residential buildings.

Hydrogen, which can be produced and stored using surplus PV capacity, offers the possibility of long-term energy storage. Metal hydride

* Corresponding author.
E-mail address: chris.drawer@tuhh.de (C. Drawer).

https://doi.org/10.1016/j.egyr.2026.109146
Received 16 September 2025; Received in revised form 4 February 2026; Accepted 26 February 2026
Available online 6 March 2026
2352-4847/© 2026 The Authors. Published by Elsevier Ltd. This is an open access article under the CC BY license (http://creativecommons.org/licenses/by/4.0/).

storage systems can safely store this highly flammable gas for any period of time; in parallel, these systems exhibit the highest volumetric energy density of all elemental hydrogen storage systems and are characterized by essentially no storage losses. Thus, this type of energy storage is ideally suited for this purpose (Drawer et al., 2024; Klopčič et al., 2023). In addition, charging metal hydride storage systems releases heat that can potentially be used in a residential building's heating system, reducing the electricity load of heat pumps.

Various investigations already address the feasibility of integrating a metal hydride storage system into an overarching energy system, primarily through theoretical simulations. One example (Möller and Krauter, 2022) uses a simulation-based approach to evaluate an energy system similar to the one proposed here – but from a purely technical perspective. Despite the comprehensive investigation of the described energy system (albeit with pressure rather than metal hydride storage), no design optimization is performed. Another study (Kumar et al., 2022) analyzes a metal hydride storage system, focusing on its thermal integration with a fuel cell and an electrolyzer. The purely technical optimization is realized for several microgrids (villages) at various wind and solar locations. A priori, this study lacks economic aspects. Another study simulates a small microgrid with a metal hydride storage system and fixed component sizes to determine electricity production costs for small laboratory devices (Kumar et al., 2019). Abdolmaleki et al. (2024) provided a simulation-based approach of integrating a metal-hydride storage in a commercial building to combine battery and metal hydride systems with an economic focus. On a much smaller scale (investigation of two representative weeks in the year), a technical analysis of a metal hydride storage system in the residential sector has already been carried out, indicating that seasonal storage is potentially feasible, without investigating this in greater depth or quantifying it in economic terms (Muñoz Robinson et al., 2024). Apart from system-integration aspects of metal hydride storage systems, the focus has so far often been on heat management, with residential buildings also being investigated (Ye et al., 2025), for example. However, the focus here is less on year-round supply and its techno-economic assessment and much more on the best possible short-term (individual days) bridging of low solar radiation for a small residential quarter. A common use for metal hydride storage systems is as a backup function, as hydrogen can be stored without loss. As in (Wang et al., 2025), these are often designed for large systems (e.g., hospitals) and are not optimized for cost-effective year-round operation, but rather for short-term bridging.

In summary, the existing literature landscape primarily focuses on simulating metal hydride storage systems in selected energy systems (e.g., laboratory or commercial buildings), with fixed capacities for the various system components and a focus on thermal management. The following aspects, in particular, are missing from the literature.

First, design optimization for a stationary application, accounting for economic and technical factors. Second, the operational optimization of such an optimized system with high temporal resolution over a more extended period of time in order to assess whether a metal hydride storage system can increase the autarky rate of a single-family house and whether a significant contribution to the heat supply within a home can be guaranteed. Third, the economic evaluation of a metal hydride storage system in order to answer the question of whether such a system is economically viable from today's perspective and/or in view of future technological and economic developments. Fourth, no study has yet examined whether integrating a metal hydride storage system into a household energy system can reduce the burden on the overall power grid.

However, given the predominantly cost-focused nature of the decision-making process involved in selecting a domestic energy system, optimization and economic analysis are essential. In addition, it is crucial to determine the temporal dynamics of energy supply and demand, necessitating the acquisition of high-resolution temporal data.

To address these gaps, this study develops an energy system model for a single-family home and applies design optimization. By minimizing total annual costs and maximizing annual autarky, the analysis assesses the role of metal hydride storage systems in single-family homes concerning key performance indicators (i.e., costs, component sizing, and energy system operation). Consistent with the identified research gaps, this work provides the following contributions.

1. A techno-economic optimization of an entire stationary single-family home energy system is carried out. In contrast to many simulation-based studies, the optimization allows for free sizing of individual components within minimum and maximum capacity limits, thereby avoiding techno-economically disadvantageous oversizing. A special feature of this model is that it is based on a “standard” single-family home and therefore takes into account the typical limitations of such homes (e.g., the maximum roof area when designing the PV system). This approach ensures that the results reflect realistic boundary conditions and are directly applicable to actual homeowner decision-making, rather than relying on idealized assumptions that may not be achievable in practice.
2. Based on high-resolution energy demand data (electricity and heat demand), design and operational optimization are carried out simultaneously, ensuring that the energy demand is met with the most optimal energy supply option at each time step. By considering an entire year, optimization in terms of autarky can be carried out in such a way that it makes the most economic sense for the overall system. Furthermore, the year-round investigation period allows seasonal storage behavior to be modeled, which is essential for assessing metal-hydride storage systems, and enables the consideration of heat integration via the metal hydride storage system.
3. The work also focuses in particular on the economic analysis of a metal hydride storage system integrated in this form. Previous research has been limited to rough cost estimates. In particular, there is little economic data available for metal hydride storage systems. The cost analysis presented in this work, which results from the optimization, not only estimates the costs of a metal hydride storage system within the framework of an integrated energy system, but also presents estimates for future developments under changing economic conditions. For the first time, a future projection is developed that allows an assessment of the extent to which the integration of metal hydride storage systems makes (economic) sense.
4. Power grid relief measures can be of great importance in a future fully renewable energy system. The extent to which metal hydride storage systems can promote this in a standard residential building is examined for the first time in this study. The increased autarky achieved by metal hydride storage can lead to a significant grid relief effect. The combined economic quantification of this increase in autarky differs significantly from previous work.

The increase in autarky presented in this paper, achieved by integrating a metal hydride storage system into standard residential buildings, has the potentially significant benefit of reducing the burden on the power grid while also increasing independence from external electricity prices that cannot be influenced. Furthermore, it can provide insights into the total costs expected to achieve these objectives.

2. Approach

To achieve the overall goal defined above and address the research questions mentioned above, an optimization-based energy system model is developed that encompasses various generation and storage technologies to meet predefined thermal and electrical energy demands for a single-family house.

The overall methodological approach is shown in Fig. 1. The modelling and optimization of this energy system is realized in Python using the Pyomo optimization tool (Bynum et al., 2021; Hart et al.,

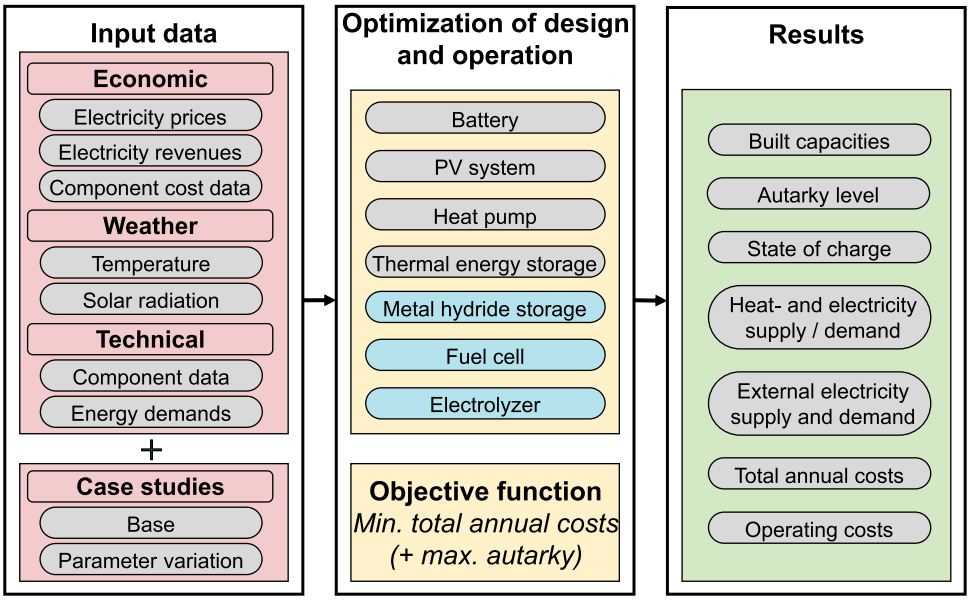

Fig. 1. Overall approach.

2011).

Based on this overall approach, several cases of the suggested energy system are defined. The corresponding input data, combined with the respective layout of the energy system, define the basis for the subsequent mixed-integer linear optimization.

The objective function for the optimization (Eq. (1)) is defined as the minimum total annual costs (TAC) consisting of the operating costs ($c_{op,t}$), the annual investment costs ($c_{CAPEX,a,n}$) and the maintenance costs ($c_{main,a,n}$) for each component ($n \in \mathcal{N}$). The operating costs include only electricity costs summed up over the considered time period ($t \in T$); they are defined as the difference between the purchase and sale of electricity.

$$\min TAC = \sum_{t\in} {}_{T} c_{op,t} + \sum_{n\in\mathcal{N}} c_{CAPEX,a,} {}_{n} + \sum_{n\in\mathcal{N}} c_{main,a,} {}_{n} \quad (1)$$

For each component (n), an annuity factor ($A_{f,n}$) (Eq. (3)) is added to calculate the yearly share of the CAPEX (capital expenditures) values for the respective component ($c_{CAPEX,n}$) throughout their economic lifetime (Eq. (2)). It includes the inflation rate ($infl$) and the nominal weighted average cost of capital ($WACC_{nom}$) as well as the deprecation period of the components (d_n) (Sens et al., 2022).

$$c_{CAPEX,a,} {}_{n} = A_{f,n} c_{CAPEX,} {}_{n} \quad (2)$$

$$A_{f,n} = \frac{\left(\frac{1+WACC_{nom}}{1+infl}\right)\left(\frac{1+WACC_{nom}}{1+infl}\right)^{d_n}}{\left(\frac{1+WACC_{nom}}{1+infl}\right)^{d_n} - 1} \quad (3)$$

The maintenance costs for each component are based on a component-specific maintenance factor.

The optimization is performed over one year with hourly detail-degree. For every timestep (t; i.e., every hour), the sum of demand ($E_{dem,b,t}$) and supply ($E_{\mathrm{sup},b,t}$) for the electricity, heat, and hydrogen bus ($b \in \mathcal{B}$) has to be zero (Eq. (4)).

$$E_{\mathrm{sup},b,t} + E_{dem,b,t} = 0, \quad \forall\ t \in T, \quad \forall\ b \in \mathcal{B} \quad (4)$$

As part of the optimization process, the optimal combination of possible energy system components is compiled, and their sizes and operating modes are determined on a cost-optimal basis.

One major focus lies on the concept of autarky. Autarky is defined here as the share of energy that can meet all demands of the respective energy system (i.e., a single-family house) without drawing on the overarching public grid. This definition is not synonymous with the term "autonomy," which means complete independence from the grid; e.g., "surplus" electricity can still be fed into the grid even when 100% autarky has been achieved.

Autarky (A) (Eq. (5)) is defined here as one minus electricity consumed from the external superior electricity grid ($E_{grid,con}$) divided by the total energy demand of the single-family house, including electricity demand (E_{elec}), heat demand via the heat pump (E_{HP}) and, if integrated within the system, electricity consumed from the electrolyzer (E_{PEMEL}).

$$A = 1 - \frac{E_{grid,con}}{E_{elec} + E_{HP} + E_{PEMEL}} \quad (5)$$

The maximum autarky (A) is determined through an iterative process that involves increasing the electricity purchase price from the public grid to a considerable extent. This, in turn, compels the optimization to reach its maximum level of autarky. Further aspects of the mathematical model are displayed in the appendix.

3. System description

The examined system represents a "standard" single-family house (SFH). The concept of the respective residential energy system is shown in Fig. 2. In general, the home energy system aims to meet a defined energy requirement (chapter 3.2.1) for electricity and heating throughout a calendar year. To achieve this, the energy system can be optimized using the components shown in Fig. 2 and described below. Heat is generated exclusively within the energy system, while electrical energy can be supplied internally via a PV system and externally from the superior electricity grid.

3.1. Components

Electricity, supplied via PV (installed on the roof) or the external power grid, is fed into the electricity bus to be used directly to meet the electricity demand of the single-family house (SFH) or indirectly for the heat bus (via a heat pump). Additionally, electricity can be stored directly in a battery or converted into hydrogen via an electrolyzer, contributing in parallel to the heat bus. The produced hydrogen is stored in a metal hydride storage system interacting with the heat bus during loading (heat supply) or unloading (heat demand). During unloading,

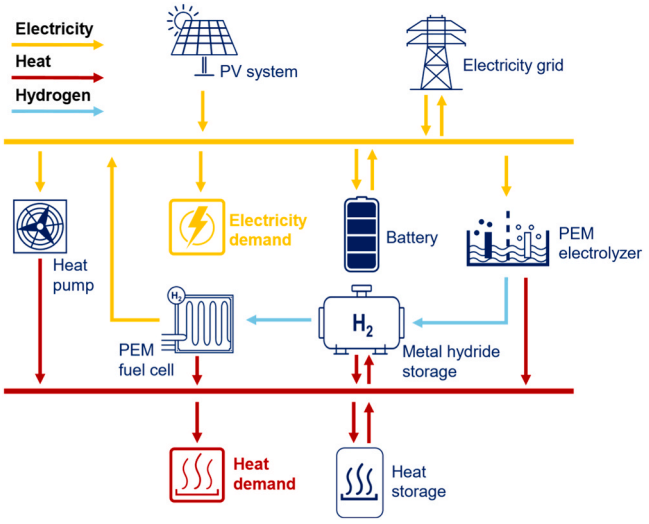

Fig. 2. System overview (PV Photovoltaic, PEM Polymer electrolyte membrane).

hydrogen is converted within a fuel cell into electricity while contributing in parallel to the heat bus. The heat bus feeds a thermal energy storage system (a hot water tank) to provide flexibility and meet the defined heat demand.

As part of the optimization process, all components shown in Fig. 2 can be used and freely optimized to meet the externally specified energy demand; the techno-economic parameters of all components are summarized in Table A. 1.

In Table 1, the optimization boundaries of all available components are listed. Since this work focuses on investigating how a metal hydride storage system can be integrated into a residential energy system, the upper limit is set significantly higher than for the other storage components to allow the effects of such an integration to be more clearly visualized.

3.1.1. Non-hydrogen components

For modelling the single-family house, non-hydrogen components are used to meet the energy requirements defined by the building standards (chapter 3.2.1). These non-hydrogen components include a "conventional" PV system for electricity supply and an air-source heat pump to meet the given heating demand. The ambient temperature and the relative PV power are taken from (Renewables.ninja, 2025) for the meteorological year 2024. The preferences for deriving these data are given in Table 2.

The mathematical formulation (Eqs. (6) and (7)) for the heat pump is

Table 1
Capacity ranges of available components for optimization (PV photovoltaic, MH metal hydride).

Component	Capacity range	References[a]
Heat pump	0 – 20 kW	(Gonschor, 2024; Krützfeldt et al., 2021)
Electrolyzer	0 – 3 kW	(Willuhn, 2024)
Fuel cell	0 – 3 kW	(Willuhn, 2024)
PV system	0 – 15 kW	(Kümpel, 2024)
Battery	0 – 25 kWh	(Orth et al., 2022)
Thermal energy storage	0 – 20 kWh	(ADAC, 2024)
MH storage[b]	0 – 2000 kWh	(Rivarolo et al., 2024)

[a] The upper limits are assumed based on the most commonly used upper limits of existing systems, based on the reference literature.

[b] The upper boundary is based on the maximum storage capacity of the medium-sized storage system of the company GKN (Rivarolo et al., 2024).

Table 2
Parameters for deriving PV data from (Renewables.ninja, 2025).

Parameter	Value
Location	53.4592° N, 9.9695° E
Tilt	35°
Azimuth	180° (South)
System loss	0.1

taken from (Sass et al., 2020). The Carnot efficiency (η_{carnot}) of the heat pump is calculated based on the ambient temperature (T_{amb}). The supply temperature of the heat pump (T_{HP}) is set to 60 °C for all heating purposes (room heating and hot water demand) (DVGW, 2004). The respective efficiency (η_{nom}) is calculated as the quotient of the factor 0.36 (Sass et al., 2020) and the Carnot efficiency.

$$\eta_{carnot} = 1 - \frac{T_{amb}}{T_{HP}} \tag{6}$$

$$\eta_{nom} = \frac{0.36}{\eta_{carnot}} \tag{7}$$

Additionally, to ensure short- to medium-term storage of excess electricity (from the PV system), a battery storage is included. To buffer heat load changes, a conventional hot-water storage tank can be installed.

3.1.2. Hydrogen components

To reduce grid electricity demand and enable a higher level of autarky, hydrogen components might be integrated into the single-family house energy system. The main objective of these components is to convert surplus electricity from the PV system, especially during summer months, into hydrogen and to convert it back into electricity during periods of high energy demand from the dwelling house when solar energy supply is low (e.g., during winter).

As conversion technologies, the (low-temperature) polymer electrolyte membrane fuel cell and electrolyzer (PEMFC and PEMEL) are selected because they are currently the most promising technologies for this type of potential application (Willuhn, 2024). Reasons include the low operating temperature (below 100 °C), the availability for small-scale applications (several kW), and market dominance (Cigolotti et al., 2021).

For hydrogen storage, a metal hydride storage (MHS) system is chosen, which enables the safe storage of hydrogen on a long-term basis; i.e., through the reaction with a metal (here: iron titanium; FeTi), hydrogen is chemically bound in a solid form without storage losses (during the storage time) (Nivedhitha et al., 2024). This type of storage offers a significant advantage over other hydrogen storage technologies that require, e.g., high pressures or very low temperatures for elementary storage of hydrogen. Despite the losses associated with such storage options, high pressure and low temperatures pose a particular safety risk (Mehr et al., 2024). Additionally, the metal hydride storage operates with moderate temperatures (up to 40 °C) and medium pressures (up to 65 bar) (Shang et al., 2022). Furthermore, the volumetric energy density is the highest for storing elemental hydrogen and is more than six times higher than that of modern lithium-ion batteries (Drawer et al., 2024; Kebede et al., 2022).

3.2. Case study definition

Different case studies are defined to evaluate how different autarky levels influence the behavior of a residential energy system for a single-family house. The six case studies defined below are separated into cases based on the current state of knowledge and up-to-date data. In addition, modifications to selected parameters that may occur in the future due to innovations and / or technological progress are addressed by varying

these parameters to examine their influence on overall results.

3.2.1. System definition

Several aspects are included within all cases defined in chapters 3.2.2 and 3.2.3. The details are outlined below.

Assumptions have to be made to ensure, on the one hand, efficient computation and, on the other hand, a feasible system (e.g., keep it linear). The most important (technical) assumptions are enumerated below.

- Thermal inertia, which might be available from former heating periods, are neglected; i.e., as soon as the ambient temperature falls below a predefined temperature limit, heating is required (heating limit temperature).
- No degradation / no efficiency losses over time of the various components are assumed.

The input for the optimization is based on economic and technical data for the year 2024. Also, measured meteorological data are used for the year 2024. The assumed developments within the parameter variation use the 2024 data as a starting point.

The single-family house is represented by an electricity and a heat demand (room heating and hot water combined). The demands are derived from the defined building standard ("KfW Efficiency House 70") and the respective house size (Calließ, 2024). The details are summed up in Table 3. The combined energy demands outlined below are shown exemplarily in Fig. 3 for one week in January and one in June.

Electricity demand. Electricity demand is derived from load profiles describing workdays, Saturdays, and Sundays (Bitterer, 1999). Based on these load profiles, the overall year is compiled. The resulting load profile is then adjusted to the defined overall demand (Table 3).

Space heating demand. The energy demand for space heating is derived from (VDI, 2007) and adjusted to heating hours (instead of days) and to the defined overall heat demand throughout a year. No heating is provided during the summer period. The target room temperature ($T_{RH,t}$) is set to 20 °C during the day and to 18 °C during the night (Eq. (8)).

$$T_{RH,t} = \begin{cases} 20 \ ^{\circ}C, & for \quad 6 \leq hour_t \leq 23 \\ 18 \ ^{\circ}C, & for \quad 0 \leq hour_t \leq 5 \end{cases} \tag{8}$$

The limit heating temperature ($T_{\mathrm{lim},t}$) is set to 15 °C; above this ambient air temperature, no heating is required. If the ambient temperature ($T_{amb,t}$) falls below the limit temperature, a temperature delta (ΔT_t) is calculated (Eq. (9)).

$$\Delta T_t = \begin{cases} T_{RH,t} - T_{amb,t}, & for \ T_{amb,t} \leq T_{\mathrm{lim}} \\ 0, & for \ T_{amb} \geq T_{\mathrm{lim}} \end{cases} \tag{9}$$

The heat demand for every timestep t ($P_{RH,t}$) is calculated by multiplying the predefined room heating demand (E_{Heat}) with the respective temperature delta and dividing it by the sum of all temperature deltas (Eq. (10)).

$$P_{RH,t} = \frac{\Delta T_t}{\sum \Delta T} E_{RH} \tag{10}$$

Hot water demand. Hot water demand curves, according to (Blatter et al., 1993), depend on the hour of the day. The respective share of the daily hot water demand ($\phi_{HW,hour}$) was measured for different households. A distinction was made between workdays, Saturdays and Sundays.

The daily heat demand ($E_{HW,day}$) is calculated by dividing the total hot water demand (E_{HW}) by the number of days in the year (d). The hourly demand ($E_{HW,t}$) is calculated by multiplying it by the daily share (Blatter et al., 1993).

$$E_{HW,day} = \frac{E_{HW}}{d} \tag{11}$$

$$E_{HW,t} = E_{HW,day} \ \phi_{HW,hour} \tag{12}$$

3.2.2. Cases

Two different case studies are defined related to the year 2024 (meteorological and economic data). These cases aim to investigate the influence of autarky on system configuration and operating behavior.

- **Base.** The external system demands (electricity and heat) can be freely met by all available components shown in Fig. 2. This is especially relevant for the hydrogen components, which are not (technically) necessary to meet the demands.
- **Base Max.** The maximum possible autarky within the predefined boundaries is assumed.

3.2.3. Parameter variation

As hydrogen components are emerging technologies, efficiency increases can be expected in the coming years. Furthermore, a decrease in the specific CAPEX values for most components is most likely (Sens et al., 2022). Additionally, changes might occur in the feed-in tariffs defined by the government and paid by the superior grid operator for the feed-in of self-generated PV electricity; most likely, these feed-in tariffs will further decrease in the coming years (Rövekamp et al., 2021).

The results of these possible developments may differ from the cases defined above. Therefore, the influence of such assumptions is examined within the scope of a parameter variation to determine how changes in the selected parameters affect the system configuration. Thus, the following parameters are changed in two steps: a minor change (*Med* cases) and a major change (*High* cases).

- Increasing the efficiency of hydrogen components
- Decreasing CAPEX for most components (excluding heat storage)
- Decreasing feed-in tariffs

The assumed reductions in investment costs and increases in efficiency vary depending on the technology (Annex Table A. 1). In both variation steps (*Med* and *High*), the system can be freely optimized and forced to reach its maximum autarky level. Table 4 summarizes the combined variations within the parameter variation.

Table 3
Single-family house details.

Parameter	Value	References
Size	150 m^2	Assumption
Electricity demand	4000 kWh/a	(Gasag, 2024)
Hot water demand	2700 kWh/a	(Umweltbundesamt, 2023)
Room heating demand	9000 kWh/a	(Calließ, 2024)
Heating period	October 1st to March 31st	Assumption
Heating limit temperature	15 °C	(VDI, 2007)
Room heating temperature day	20 °C	(Umweltbundesamt, 2023)
Room heating temperature night	18 °C	(Umweltbundesamt, 2023)

4. Results and discussion

The following chapter analyses the results of all cases from a techno-economic perspective.

4.1. Cases

The results of the respective optimization runs are assessed by evaluating the following parameters.

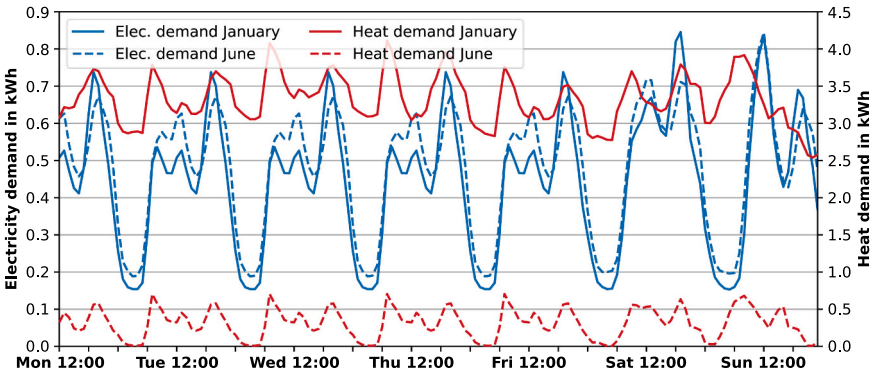

Fig. 3. Exemplary energy demands in January and in June (Elec. Electricity).

Table 4
Case definition within the parameter variation.

Cases	CAPEX	Efficiencies hydrogen components	Feed-in tariffs	Autarky
Base	Base	Base	Base	Free
Base Max	Base	Base	Base	Max
Med	↓ Med	↑ Med	↓ Med	Free
Med Max	↓ Med	↑ Med	↓ Med	Max
High	↓↓ High	↑↑ High	↓↓ High	Free
High Max	↓↓ High	↑↑ High	↓↓ High	Max

- Built capacities of all components
- Level of autarky (i.e., independence from external energy supply)
- State of charge of the respective energy storages
- Supply and demand of electricity
- Supply and demand of heat energy
- Total annual costs
- Operating costs

4.1.1. Capacities

The capacities resulting from the *Base* and *Base Max* cases are shown in Fig. 4.

The *Base* case is optimized freely (i.e., no restrictions are imposed on the autarky or the amount of externally supplied electricity to the proposed energy system). The optimization of the defined energy system for the conditions defined within the *Base* case yields the following capacities: a PV system with a maximum capacity of 15 kW, a battery with a capacity of 3.9 kWh, a thermal energy storage system with a capacity of 18.3 kWh, and a heat pump with a capacity of 3.8 kW. Consequently, the system has been designed to prioritize cost-effectiveness, resulting in the exclusion of hydrogen components.

For the *Base Max* case, the external energy supply can be reduced to 2.45 MWh, which is 55% of the *Base* case external energy supply. The non-hydrogen components are built to their maximum capacity, except for the heat pump with 8.2 kW (i.e., the PV system with 15 kW, the battery with 25 kWh, and the thermal energy storage with 20 kWh). The hydrogen components are designed with 1.6 kW for the electrolyzer and 1.3 kW for the fuel cell. The metal hydride storage system has been built to its maximum capacity of 2 MWh. In particular, all storage systems are dimensioned to their maximum permissible size in order to maximize the storage of self-generated electricity and autarky.

The hydrogen components installed additionally in the *Base Max* case, compared to the *Base* case, and the maximum utilization of storage capacities indicate that a further increase in the respective autarky level would be possible with higher storage system limits.

4.1.2. Autarky

Fig. 5 compares the total and monthly degrees of autarky for both cases on a monthly basis over the year and in total.

Within the *Base* case, an annual autarky level of 52% is achieved. By analyzing autarky on a monthly basis, a clear correlation between autarky levels and monthly variations in sunlight hours becomes apparent. This is the main reason why the monthly autarky levels decline during the winter months, reaching a minimum in December and January with 15% and 22%, respectively. Conversely, the summer months demonstrate a marked increase in autarky levels, reaching a maximum of 100% during the peak summer period covering the time period from May to August. This clearly correlates with the high PV

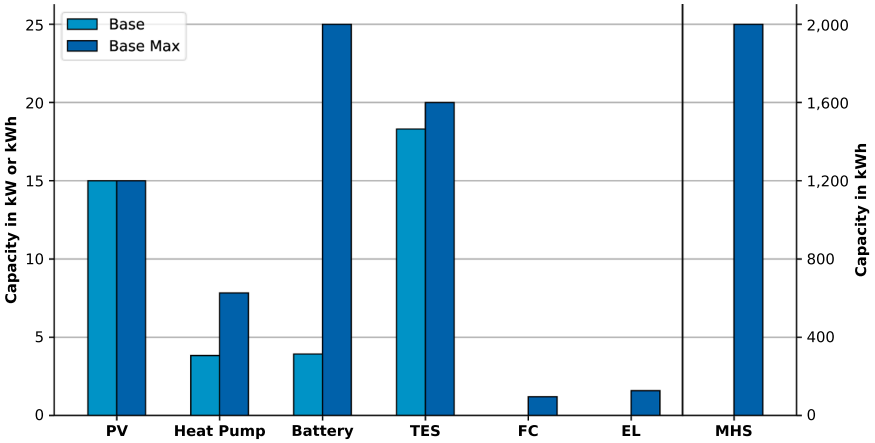

Fig. 4. Built capacities, cases *Base* and *Base Max* (PV Photovoltaic, TES Thermal energy storage, FC Fuel cell, EL Electrolyzer, MHS Metal hydride storage).

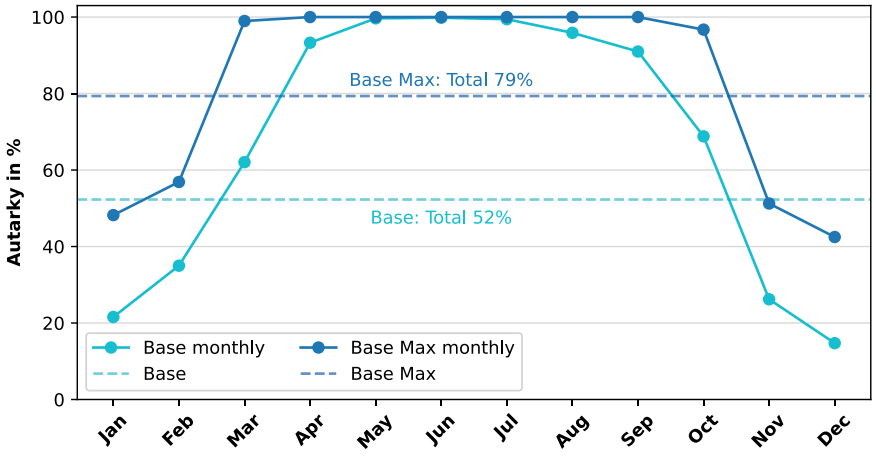

Fig. 5. Autarky level during the year, cases *Base* and *Base Max*.

supply, which more than covers electricity demand in the summer. The most significant increase is evident from February to March, with an increase of almost 30%-points. Conversely, a notable drop is observed from October to November, with a decrease of more than 40%-points, when solar radiation and the electrical energy it supplies increasingly diminish.

The maximum achievable autarky value for the *Base Max* layout is 79% over the year, with 100% autarky from April to September. After October, the autarky level drops significantly because efficiency losses during hydrogen conversion prevent the hydrogen components from achieving a higher autarky within the given limit of available hydrogen storage capacity. One major difference compared to the *Base* case is the much higher autarky level during the winter months, e.g., 42% in December and 48% in January.

Compared to the *Base* case, the metal hydride storage (in combination with the hydrogen conversion components) significantly increases the autarky of the *Base Max* case by enabling seasonal energy storage, unlike the battery, which allows only daily storage.

The *Base* autarky with a level of 52% is comparable to values in literature for such a layout of "conventional" PV-battery systems for residential energy systems (e.g., (Ciocia et al., 2021; Gudmunds et al., 2020)).

4.1.3. Electricity

The effects of the system designs on electricity consumption and supply are shown in Fig. 6.

For the *Base* case (Fig. 6, left), the house-only electrical load (dashed line) shows that more energy is supplied than consumed over the course of a year, as evidenced by the PV plant. But even in summer, with high PV electricity generation, only a small amount is stored in the battery. The greater share of the generated PV electricity is fed into the superior electricity grid, generating revenue through its sale. The yearly electricity consumption from the grid in the *Base case* is 10.79 MWh. Since the monthly energy demand and the monthly energy supply of the battery are very similar, it can be assumed that the battery does not perform seasonal energy storage.

In the *Base Max* case (Fig. 6, right), the electrolyzer operates primarily in the summer, and the fuel cell mostly in the winter. It indicates that a significant amount of hydrogen is produced during summer and stored until winter; i.e., there is less / no continuous charging and discharging on a daily or weekly basis. The metal hydride storage is mainly used for seasonal energy storage, shifting energy from summer to winter. But even with this high capacity of the metal hydride storage system, on days with high solar radiation, much more PV electricity is generated; i.e., the battery capacity is insufficient to store this surplus energy, and

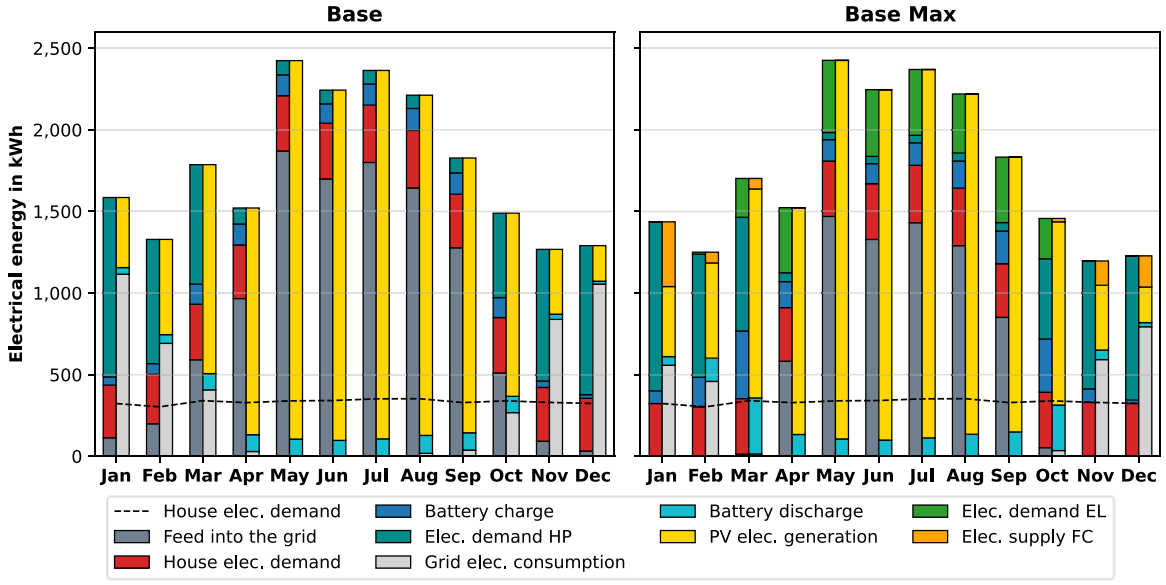

Fig. 6. Electrical energy supply and demand over the year, cases *Base* and *Base Max* (consumption: left bar, supply: right bar; Elec. Electricity, HP Heat pump, PV Photovoltaic, EL Electrolyzer, FC Fuel cell).

even the electrolyzer cannot take up all the remaining electricity and convert it into hydrogen. As a result, a significant amount of electricity continues to be fed into the overarching grid, albeit at a substantially lower level than in the *Base* case.

When comparing the *Base* and *Base Max* cases, seasonal energy storage is enabled in the *Base Max* case. It can therefore improve the degree of autarky, particularly in winter, thereby increasing it over the course of the year. However, the feed-in of surplus electricity generated by the PV system in summer remains a significant part of the electricity balance.

4.1.4. Heat

Heat supply and demand are shown in Fig. 7. The total heat demand (room heating and hot water) is significantly higher in winter than in summer. The reason is that during the summer, only hot water is required.

For the *Base* case (Fig. 7, left), the charging and discharging of the hot water tank and the heat pump energy during the summer months exhibit a high degree of similarity in terms of energy quantity; i.e., during periods of less or no solar radiation, the surplus PV energy is utilized to charge the thermal energy storage through the heat pump. This stored energy can subsequently be utilized during nocturnal hours, thereby ensuring a consistent and reliable energy supply. Conversely, during the winter season, thermal energy storage utilization is minimal, leading to a predominant reliance on heat pumps to meet thermal energy demands.

The *Base Max* case (Fig. 7, right) shows only a small influence of the fuel cell and electrolyzer. During the summer season, a part of the hot water demand can be covered by the hydrogen converters' "waste" heat, but especially during the winter term, a significant impact on the heating system cannot be investigated (i.e., the impact is too low compared to the required heat demand). The influence of the metal hydride storage system is even less significant. During the hydrogen storage, discharge, and utilization of the fuel cell, only a minor effect on the heating system was observed in January. Thus, integrating a metal hydride storage system does not make a significant contribution to the heating system under the assumptions made here.

A comparison of the two cases reveals that the pattern of heat demand and supply remains relatively unaltered. Hydrogen components of this size and a metal hydride storage system with the assumed storage parameters (enthalpy, operating temperature) do not replace the heat pump for the primary heat supply. This is because the selected hydrogen components operate at low temperatures and cannot supply sufficient thermal energy in small built sizes (in the case of fuel cells and electrolyzers). For a greater impact (i.e., to cover the heat demand), larger capacities of fuel cells and electrolyzers are required or even components with higher operating temperature levels are needed.

4.1.5. State of charge

To gain a more profound understanding of the charging and discharging behavior of the battery, the hot water storage and the metal hydride storage, the average daily means of the state of charge levels over the year are analyzed (Fig. 8).

In both cases (*Base* and *Base Max*), the thermal energy storage and the battery function as short-term storage on a daily/hourly basis. These components primarily store energy generated during the day by the PV system. Additionally, the thermal energy storage is less utilized during the summer and more during the transitional seasons. This discrepancy could be attributed to the fact that, during the summer months, large amounts of stored hot water are typically not required, thereby reducing demand for full storage capacity.

In the *Base* case (Fig. 8, top), no seasonal storage is observed, as indicated by the autarky results and by electricity supply and demand. Since the objective function of the *Base* case is economically justified, surplus energy is not stored in the long term but fed into the superior electricity grid, as the feed-in tariff assumed here enforces this as the economically more viable option.

For the *Base Max* case (Fig. 8, bottom), the assumed seasonal storage of the metal hydride system, as indicated by the focus on electricity supply and demand, is clearly visible. While storage discharges slowly but steadily at the beginning of the year, it is charged continuously during the summer months, starting already in April. Furthermore, a direct comparison reveals that the battery capacity is more used in the *Base* case in summer. In contrast, in the *Base Max* case, the optimization focuses not only on costs but also on autarky and reduced external energy demand, so it is not fully required. The same is true for the thermal energy storage. However, since the CAPEX for this storage type are very low (Table A. 1), it does not require full capacity use to be cost-effective.

These results show that seasonal storage achieved by metal hydride storage is an important factor in increasing the autarky level of the house energy system.

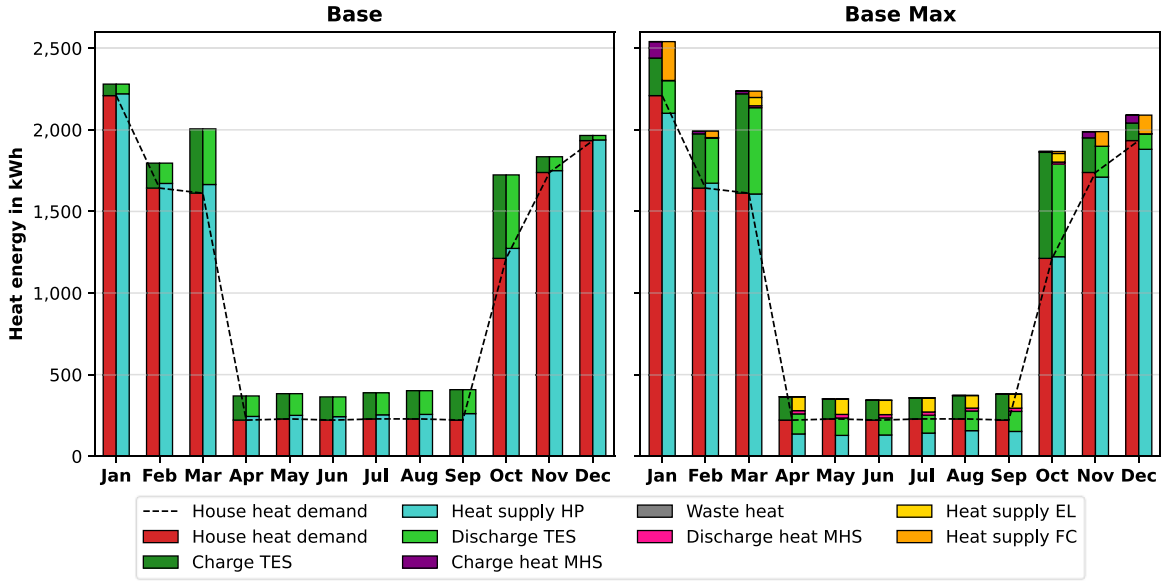

Fig. 7. Heat energy supply and demand over the year, cases *Base* and *Base Max* (consumption: left bar, supply: right bar; TES Thermal energy storage, HP Heat pump, MHS Metal hydride storage, EL Electrolyzer, FC Fuel cell).

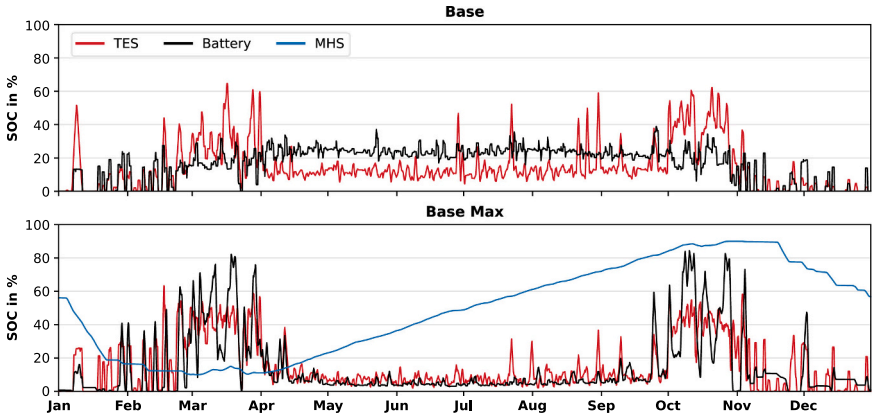

Fig. 8. State of charge of over one year, cases *Base* and *Base Max* (TES Thermal energy storage, MHS Metal hydride storage).

4.1.6. Total annual costs

The total annual costs (TAC) describe the investment costs distributed annually, the annual maintenance costs, and the operating costs (only electricity costs). Fig. 9 shows the total annual costs for the *Base* and *Base Max* cases, along with the corresponding built capacities.

In the *Base* case, the maximum capacity is allocated to the thermal energy storage, and the associated costs are minimal. The annual costs associated with electricity demand from the external grid (operating costs) account for 37% of total annual costs. The annualized investment costs for the PV system also have a significant influence, accounting for about 35% of the total annual costs.

The primary cost driver associated with the forced integration of hydrogen components within the *Base Max* case is the metal hydride storage, which is built with a very high storage capacity and accounts for 41% of the total annual costs. Electricity costs can be reduced to 4%. Although the CAPEX for the electrolyzer and the fuel cell are assumed to be high per kW compared to the non-hydrogen components, their share of the total annual costs is not significant since only a limited capacity is built. To achieve the maximum achievable autarky of 79% under the given constraints (i.e., the predefined maximum installable capacities), the total annual costs sum to 11,386 €, about a factor of 4.4 higher than the *Base* costs.

In summary, integrating a metal hydride storage system with the necessary peripheral devices (i.e., a fuel cell and an electrolyzer) results in a significant increase in costs relative to the base case. To better compare total annual costs, the overall yearly costs for the *Base* and *Base Max* cases are broken down into monthly cost shares (Fig. 10). Compared with conventional electricity and heat procurement, a similar pattern is observed over the course of the year. Costs are high in winter and low in summer. In June and July, the costs for *Base* are almost zero, and in May, there are even revenues due to the high electricity feed-in. In the case of *Base Max*, costs also fall during the transition to summer. However, the monthly impact (at a much higher level) is less significant because CAPEX accounts for a much higher proportion of total annual costs than operating costs.

4.1.7. Operating costs

To understand the impact of operating costs in both cases, Fig. 11 shows monthly operating costs over the year. The patterns in both cases are similar, although the difference between winter and summer is much greater in the *Base* case. Operating costs in January are around 440 €, while a revenue of 141 € is generated in May. It shows a high level of interaction with the superior grid in both directions, through supply and feed-in.

The difference between electricity purchase in winter and sales in summer is less significant within the *Base Max* case. In January,

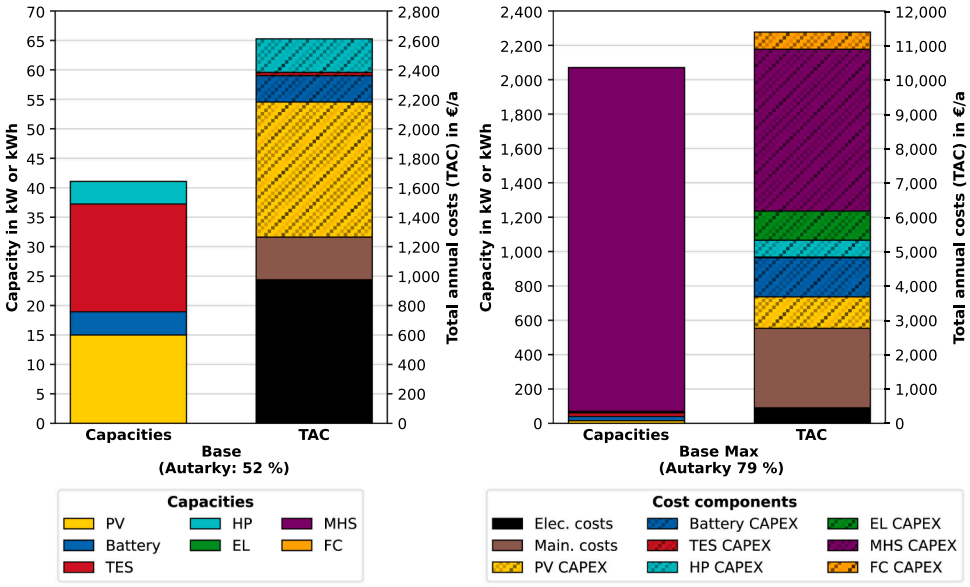

Fig. 9. Total annual costs and built capacities, cases *Base* and *Base Max* (TAC Total annual costs, PV Photovoltaic, HP Heat pump, TES Thermal energy storage, MHS Metal hydride storage, FC Fuel cell, EL Electrolyzer, Elec. Electricity, Main. Maintenance, CAPEX Capital expenditures).

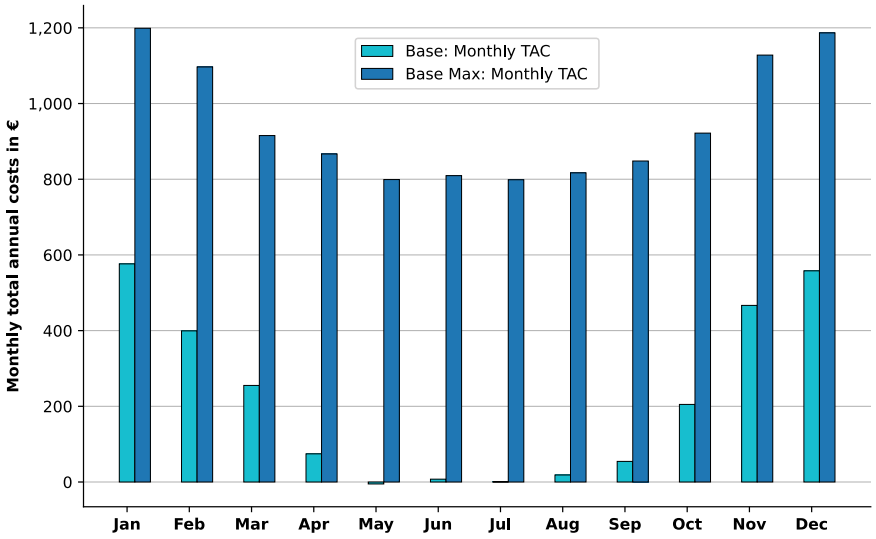

Fig. 10. Comparison of monthly total annual costs, cases *Base* and *Base Max* (TAC Total annual costs).

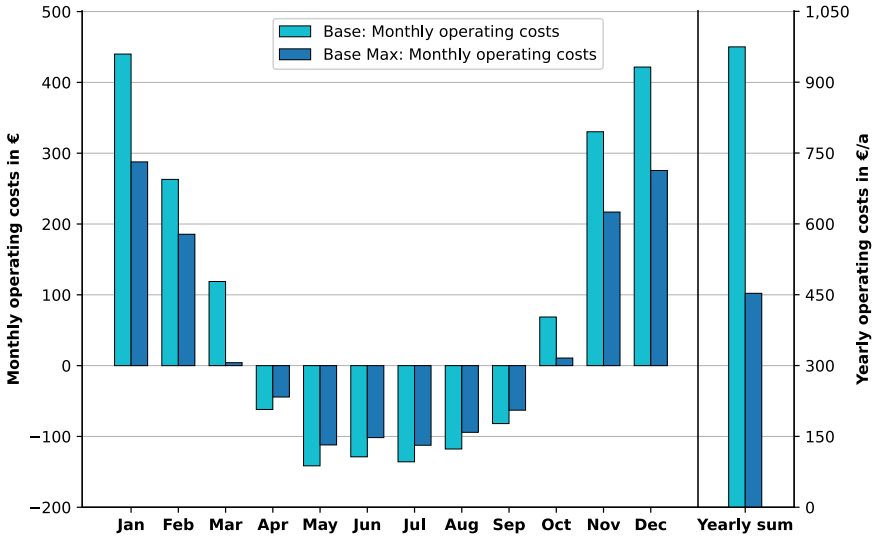

Fig. 11. Operating costs, cases *Base* and *Base Max*.

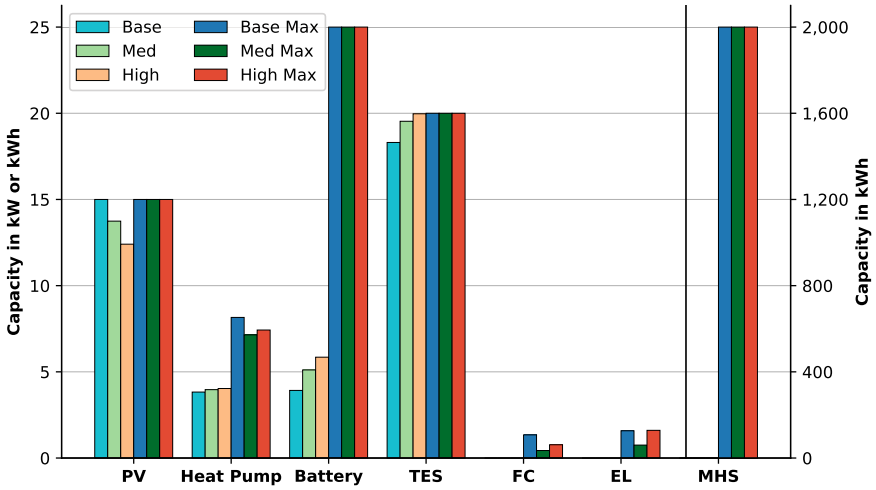

Fig. 12. Built capacities parameter variation (PV Photovoltaic, TES Thermal energy storage, FC Fuel cell, EL Electrolyzer, MHS Metal hydride storage).

operating costs amount to 288 €, which is ca. 35% less than in the *Base* case. The revenue generated in summer is also lower than in the *Base* case, with a maximum of 112 € in July.

Comparing the annual total operating costs (defined as the sum of electricity costs and revenues from electricity sales) of both cases, the *Base Max* case shows less than half of the operating costs of the *Base* case. This fact supports the analysis that the *Base Max* case has much greater independence from the superior power grid than the *Base* case.

4.2. Parameter variation

Assuming increasing efficiency and decreasing specific CAPEX in the future, as well as decreasing feed-in tariffs, leads to the following results. To make the consequences of such variations (Table 4) apparent, unlike for the *Base* and *Base Max* cases, only selected techno-economic parameters are analyzed and discussed for the parameter variation (chapter 4.2).

4.2.1. Capacities

The built capacities (Fig. 12) are similar to those in the *Base* case.

Different than in the *Base* case, in the *Med* case, and in the *High* case, the PV system is not built to its maximum capacity; i.e., a smaller PV system is realized (13.7 kW in the *Med* case and 12.4 kW in the *High* case). The installed battery has a slightly higher capacity (5.1 kWh in the *Med* case and 5.9 kWh in the *High* case) than in the *Base* case (4 kWh). This is because investment costs for batteries are assumed to be significantly lower in the High case, and feed-in tariffs will no longer be paid (chapter 3.2). The thermal energy storage and heat pump capacities in the *Med* and *High* cases are comparable to those in the *Base* case, with the latter exhibiting a slightly lower capacity of ca. 4 kW. Due to economic reasons, no hydrogen components are built in these cases. In summary, this means higher storage capacities and lower electricity generation capacities.

A significant difference can be observed when evaluating the cases *Med Max* and *High Max*. The capacities of the PV system, the battery, and the thermal energy storage are set to their maximum values. The heat pumps are built with capacities of about 7.1 kW (*Med Max*) and 7.4 kW (*High Max*), which are considerably higher than in the freely optimized cases. In the *Med Max* and *High Max* cases, the metal hydride storage is built to its maximum predefined boundary (i.e., maximum allowed storage capacity). In contrast, the fuel cell in both cases and the electrolyzer in the *Med Max* case are built below 1 kW. In the *High Max* case, however, the electrolyzer is built at 1.6 kW.

4.2.2. Autarky

Within the parameter variations, the lowest achievable autarky when optimizing the overall system solely from an economic point of view is 53% in the *Med* case (Fig. 13), which is slightly higher than in the *Base* case; this is also true on a monthly basis. The highest level of autarky, around 80%, can be achieved in the most progressive case with maximum autarky (*High Max*). This highest autarky degree is only 1%-point higher compared to the *Base Max* case and is far from 100% autarky. The main reason for this is attributed to high efficiency losses during the conversion steps of electricity into hydrogen and into the storage, as well as back into gaseous hydrogen and electricity.

Higher efficiencies lead only to a slightly higher autarky level in the *High* case compared to the *Med* Case. In the *High Max* case, 100% monthly autarky can be achieved from March to September. However, it drops significantly in October (*Med* and *High*) and November (*Med Max* and *High Max*) and reaches its lowest values in December and January.

Therefore, even future developments (e.g., further increasing efficiency values) are not expected to lead to significantly higher autarky levels for the proposed system. Overall, the conversion losses from electricity to hydrogen and vice versa are very high and thus require, for higher autarky levels, a clearly larger PV system as well as higher storage capacities to be filled during summer.

4.2.3. Feed-in and self-consumption

While the potential for future efficiency enhancements may only modestly enhance the system's autarky, the underlying principle of the initial research inquiry, namely the mitigation of grid load, is indeed attainable. Fig. 14 shows a comparison of all cases in terms of electricity self-consumption and feed-in to the superior grid over the course of one year. The *Base* case has the highest electricity consumption at 4.46 MWh, while the *High Max* case shows the lowest at 2.29 MWh, resulting in a reduction of about 50%. A clear shift can be seen from the freely optimizable cases (*Base*, *Med*, *High*) to the *Max* cases, as higher autarky levels, i.e., greater self-consumption of electricity, naturally reduce grid power consumption.

Another significant reduction can be achieved by examining the feed-in to the grid values, which are reduced from 10.79 MWh (*Base*) to 7.01 MWh (*Base Max*), representing a reduction of about 35%. In particular, there is a significant reduction in grid feed-in across the *Base*, *Med*, and *Max* cases. In conjunction with lower PV capacities and larger battery storage, the overproduction of electricity becomes less profitable, which is why less is produced and more is charged into the battery storage. Additionally, feed-in is mainly reduced during the summer, which relieves the grid most during periods of high PV electricity output.

In summary, integrating a metal hydride storage system can reduce grid loads; however, it necessarily entails high conversion losses.

4.2.4. Total annual costs

A detailed examination of the freely optimized *Med* and *High* cases (Fig. 15, left) reveals that the aggregate costs are closely aligned with the

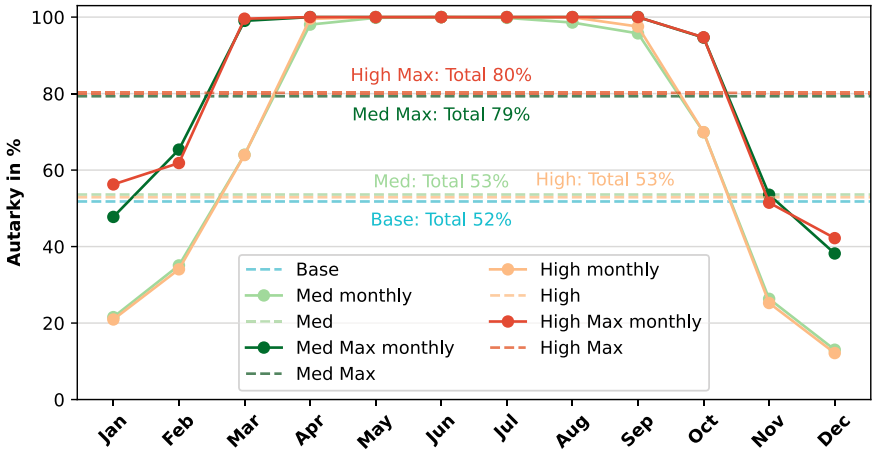

Fig. 13. Autarky level during the year, parameter variation.

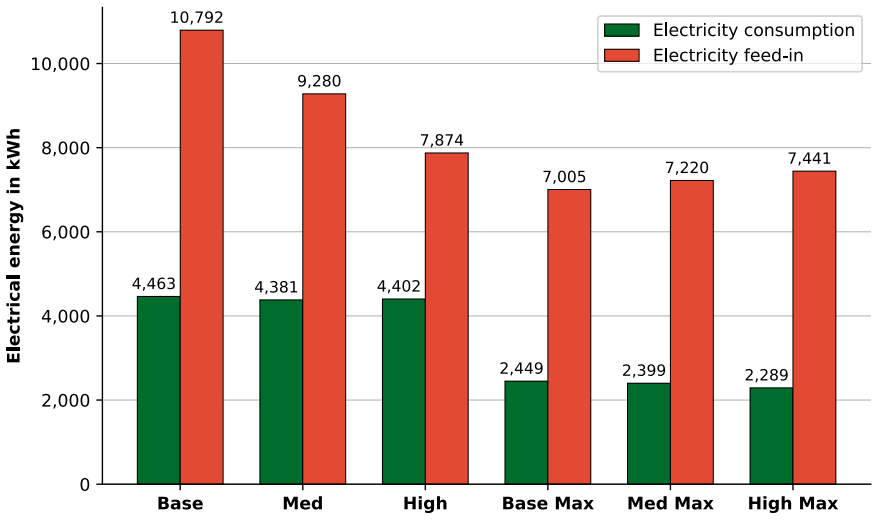

Fig. 14. Electricity consumption and feed-in, all cases.

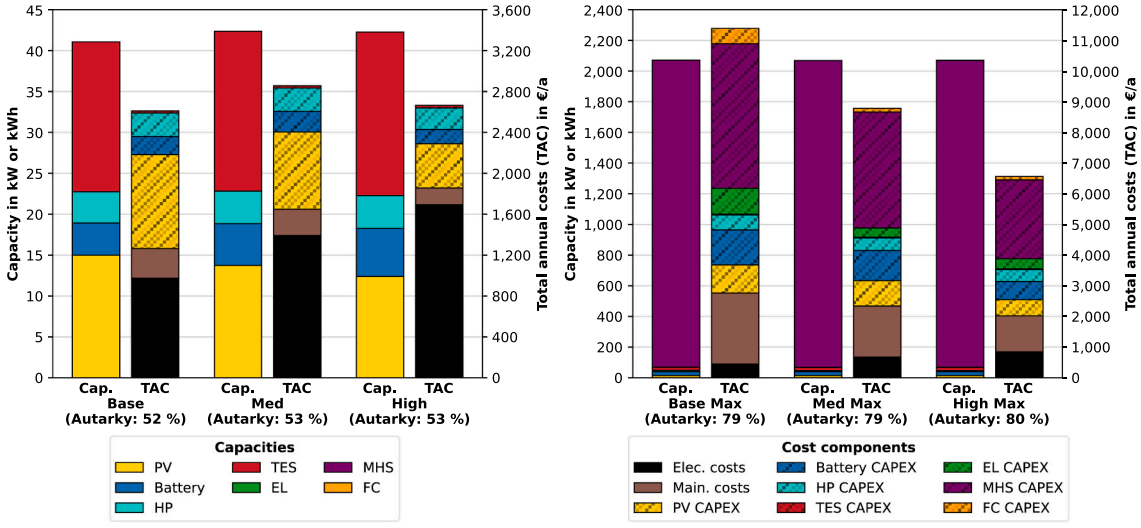

Fig. 15. Total annual costs, parameter variation.

Base case costs. In the *Med* case, the annual costs amount to 2856 €, which are higher than in the *Base* case. In the *High* case, the annual costs amount to 2663 €, which is still 2% higher compared to the *Base* case.

The reason for this connection is that the CAPEX reduction in the *Med* case does not offset the increasing operating costs (due to lower revenues from lower feed-in tariffs), which account for about 49% of total annual costs. Even with significant CAPEX reductions (*High*) (Annex Table A. 1), the total annual costs decrease only modestly, with operating costs accounting for about 64% of the total. As in the definition of the assumed cases, *Med* and *High*, these two effects (future CAPEX decline and decline in feed-in tariffs) offset each other, with reimbursements from electricity sales having a stronger effect.

Looking at the *Max* cases (Fig. 15, right), the costs for metal hydride storage dominate, as in the *Base Max* case. However, total annual cost reductions of 23% in the *Med Max* case and 42% in the *High Max* case, compared to the *Base Max* case, are projected. The share of operating costs in the case *High Max* can be reduced to 13%.

In summary, unlike the cases *Base* and *Base Max*, reducing operating costs is a key factor in reducing overall costs. Even though the maximum autarky case will incur higher expenditures in the *High* cases when compared to cost-effective systems, substantial operating cost reductions can be attained by increasing autarky levels. However, the financial implications of a maximally autarkic system reliant on metal hydride storage in the *High* cases will remain 2.5 times greater than those of a system optimized solely for cost-effectiveness. Consequently, it is not realistic to anticipate cost-optimized operation with the utmost autarky using a metal hydride system, even in the most progressive *Max*

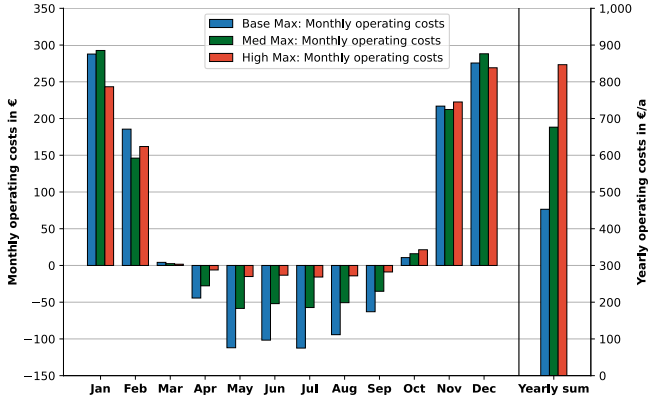

Fig. 16. Operating costs, cases *Base Max*, *Med Max* and *High Max*.

case.

4.2.5. Operating costs

The isolated impact of reduced feed-in tariffs can be observed in Fig. 16 when comparing the *Max* cases.

Although electricity consumption from the grid is very similar in the *Max* cases (Fig. 14), operating costs vary greatly. While the operating costs for the *Base Max* case incur costs in the winter season and generate revenue through sales in the summer, a significant reduction is observed in the *Med* case. Since very low feed-in tariffs are assumed for the *High Max* case, mostly costs (mainly in winter) are incurred, and small revenue is generated in summer. This leads to an increase of about 80% in electricity costs for the *High Max* case compared to the *Base Max* case.

This shows that even though feed-in of surplus electricity is mainly relevant in summer for generating revenue, the decline in feed-in tariffs has a significant impact on overall operating costs.

4.3. Verification of the results

As part of a plausibility check, it should be discussed to what extent the results obtained correspond to the behavior of real systems and to what extent deviations in individual parameters impair the robustness of the findings.

The concept presented in this work and the techno-economic optimization focused on maximizing autarky (from the higher-level power grid) have not yet been the focus of research. However, the plausibility, i.e., the fundamental meaningfulness of the results, can be checked. On the one hand, the components integrated into the *Base* case are part of modern house energy systems and can therefore be compared with other literature. On the other hand, a parameter variation was carried out within the scope of the parameter study, which shows both the robustness of the results and the most important influencing factors.

4.3.1. Comparison to literature

As already mentioned in Section 4.1, the autarky determined in the *Base* case is comparable in order of magnitude to the approximately 50% reported in the literature (Ciocia et al., 2021; Gudmunds et al., 2020). The studies mentioned included a combination of PV and battery (Ciocia et al., 2021) or a combination of PV and a comparison of stationary and mobile batteries in the form of an electric car (Gudmunds et al., 2020). In (Gudmunds et al., 2020), an autarky of up to 43% was achieved with a stationary system, and in (Ciocia et al., 2021), a value of 52–65%, depending on the size and type of the battery and the size of the PV system. This is in the same order of magnitude as the 52% autarky determined in this study for the *Base* case.

The *Base* case can also be used as a benchmark for costs. This results in a cost-optimized system within the defined limits, consisting of the components heat pump, battery and heat storage, and PV system. Its structure is comparable to, e.g., the system configuration in (Meriläinen et al., 2023), which was determined to be the cost-optimized system for a Scandinavian townhouse. This also underscores the basic assumption of this work that a purely cost-optimized system excludes the possible integration of hydrogen components as part of the optimization process, which necessitates the addition of a further constraint to the system in the form of the autarky to be achieved.

Further studies dealing with the design of batteries and heat pumps also show that the assumed electricity price is decisive for the cost-optimality and design of such systems (Rieck et al., 2025; Wüllhorst et al., 2024). The electricity price assumed in this work is from 2024; it is not expected that the electricity price in Germany will fall significantly in the coming years (Liebensteiner et al., 2025). The model's basic assumptions can therefore be considered sound. The reason why the cost-optimized system configuration does not contain any hydrogen components in the *Base* case is due to the still-high specific investment costs and the high conversion losses when converting electricity to hydrogen and back.

In (Muñoz Robinson et al., 2024), a simplified model, two representative weeks, one in winter and one in summer, were examined using a metal hydride storage tank in a residential building. Only the technical aspects of the two weeks were considered. The electricity consumption from the grid and the supply via PV in these two weeks are comparable to the results of this study. The study also confirms the heat pump's predominant contribution in winter and the subordinate contribution of the hydrogen components.

4.3.2. Uncertainty analysis

A parameter variation was performed to determine the extent to which the system's robustness/sensitivity is influenced by the assumptions made. The varied parameters include the specific investment costs of the components, their efficiency, and the assumed feed-in tariff. The parameter variation was carried out in two steps: minor (*Med* cases) and major (*High* cases) changes in values.

The selection of specific investment costs is subject to uncertainties, especially for hydrogen components that are still under development. In addition, the systems considered here have not yet been used in single-family homes on this scale. For this reason, a reduction in costs can generally be expected in the future. The situation is similar regarding the assumed efficiencies, as all technologies, except the heat storage system, are still under development. Therefore, an increase in efficiencies can be expected. The legislative framework also creates significant uncertainties. Possible subsidies or potential incentives that support the grid-relieving behavior of the energy system examined here have not been assumed. However, a reduction in the feed-in tariff paid is highly likely in the future (Rövekamp et al., 2021), which is why it has been reduced accordingly in two steps.

The influence of this parameter variation on the technical and economic results presented below can provide an indication of the system's robustness.

The economic results of this parameter variation show that potential cost reductions can be achieved by integrating the autarky condition, but that, compared to the conventional *Base* case, no purely economically cost-optimal scenario occurs. The assumed *Base* case can therefore be considered a worst-case scenario (in terms of expected costs). At the same time, there are hardly any changes in costs in the purely techno-economic cases (*Base*, *Med*, *High*); the total annual cost level remains relatively constant. Even with significant improvements (*High*) in the techno-economic parameters of hydrogen components, the system configuration changes little in the cost-optimized case, and no hydrogen is used. It follows that metal hydride storage systems are therefore unlikely to be economically competitive in the future without subsidies.

Regarding the technical results, the influence of the varied parameters is presumably due primarily to the reduced feed-in tariff in the *Med* and *High* cases. In particular, the feed-in of electricity into the higher-level power grid is reduced in the purely economically optimized cases (without autarky conditions), as this is less economically viable. When maximum autarky is enforced (*Max* cases), the energy to be fed into the grid hardly changes, as it has already been reduced to a minimum. Furthermore, despite improved techno-economic parameters of the components, autarky increases only very slightly (from 79% to 80%). The limiting factor is therefore more likely to be external conditions imposed by the house (e.g., usable roof area for a PV system).

In summary, variations in individual parameters result in changes in both economic and technical results. However, this does not change the core findings of the study: metal hydride storage systems can increase the autarky level of a home energy system, thereby reducing the load on the power grid, but the economic operation of such a system is most likely only possible through policy incentives, despite future (potentially improving) framework conditions concerning the technical and economic parameters of the system components considered here. The most decisive influence on the system was attributed less to technical and economic developments/changes in system components and more to changing feed-in tariffs, which are driven solely by regulatory factors.

5. Conclusions

This optimization-based work aims to perform a techno-economic evaluation of an energy system for a single-family house, based on a metal hydride hydrogen storage system in combination with an electricity-based heating system (i.e., an air-source heat pump) and a PV system providing the necessary electrical energy. The mixed-integer linear optimization of the respective residential energy system is performed to analyze the system in terms of energy design (i.e., component sizes) and operation (i.e., electricity and heat supply/demand), as well as its economic parameters, such as total annual costs. The subsequent key results can be summarized as follows.

- The main technical goal of maximizing autarky, based on hydrogen components (converters: fuel cell, electrolyzer; storage: metal hydride), could be partially achieved by reaching an autarky level of roughly 80%, limited by the maximum allowable installable hydrogen storage capacity. This autarky level represents a clear improvement compared to the autarky achievable in the *Base* case, where no seasonal hydrogen storage is assumed, which is 52%. Nevertheless, if the upper limits for energy storage and the PV system defined here are raised, achieving 100% autarky is most likely.

- With hydrogen conversion components and an adequate size of the metal hydride storage tank, significant reductions in the feed-in of the produced PV electricity into the superior public grid can be achieved; with the assumed definitions realized here, a reduction of about 35% over one year is easily possible. Similar results can be obtained for the consumption; between the *Base* case and the most progressive case (*High Max*), there is even a reduction of about half.
- The goal of a significant contribution of the metal hydride storage system to the heating system was not achieved. This is partly attributable to the low-temperature components that were deliberately selected (e.g., for safety reasons) for such a home system. Conversely, only a portion of the components' energy output can be utilized for heat extraction, and 100% utilization is not feasible a priori.
- The enforced autarky of close to 80% for today's system (*Base Max* case) leads to significantly higher total annual costs. They are ca. 4.4 times higher than the base-case costs (i.e., no seasonal storage). The primary factor contributing to these clearly elevated costs is CAPEX associated with the hydrogen components, including metal hydride storage. Notably, the hydrogen storage component, which possesses the largest storage capacity, accounts for ca. 41% of the total annual costs. In this context, the economic viability of the proposed house system, incorporating an integrated metal hydride storage system, is not given from a present-day perspective.

- The economic analysis of minor (*Med* cases) and major (*High* cases) changes in selected parameters shows, on the one hand, a slight increase in total annual costs when optimization is based solely on costs (+9% in the *Med* case). This is due to declining feed-in tariffs, which are assumed. On the other hand, however, a significant cost reduction can be observed with a cost-autarky-optimized system, with total annual costs amounting to 6560 €. However, with a factor of 2.5, this value in the most progressive case (*High Max*) is not as far above the cost-optimal system as it is in the *Base* case; a reduction in this gap and thus an increase in the attractiveness of such a system might be conceivable through further cost decrease of such systems (or higher costs of electricity from the superior grid).

In summary, from a purely cost optimization perspective, a metal hydride storage system is not a promising solution for a home storage system. However, if additional (technical) factors are taken into account (such as autarky or grid relief), the future integration of such systems is conceivable. This is due in part to the expected sharp decline in specific CAPEX in the future. In addition, external factors could potentially reduce the cost gap and thus increase the attractiveness of an autarky-maximized system through (financial, e.g., tax) incentives or subsidies; future variable electricity prices in particular could be a factor here.

Given the sensible increase in autarky identified here from a technical and, in part, economic perspective, a more in-depth analysis of the potential integration of the metal hydride storage technology proposed here, including the necessary hydrogen conversion technologies, at a more centralized level (e.g., at the residential neighborhood level), is a future open research question that appears worthwhile to investigate.

CRediT authorship contribution statement

Chris Drawer: Writing – original draft, Validation, Software, Methodology, Investigation, Formal analysis, Conceptualization. **Luka Bornemann:** Writing – review & editing, Validation, Software, Conceptualization. **Martin Kaltschmitt:** Writing – review & editing, Supervision, Methodology.

Funding

This work was funded by the German Federal Ministry of Research, Technology and Space (BMFTR) via the project HyPoKo (Grant no. 03SF0657C). Publishing fees supported by Funding Programme Open Access Publishing of Hamburg University of Technology (TUHH).

Declaration of Competing Interest

The authors declare that they have no known competing financial interests or personal relationships that could have appeared to influence the work reported in this paper.

Appendix

Mathematical formulation

Crucial aspects of the mathematical model are displayed below. The incorporated input parameters are shown in Table A. 1. Further information is provided in (Sass et al., 2020) and (Bornemann et al., 2025).

As described in Eq. (A1), the investment costs for a component (I_c) with size (Q_c) is calculated with the economy of scale formula, based on investment costs (I_c^{ref}) for a reference size (Q_c^{ref}) to the power of a component-specific scale factor (M_c).

$$\boldsymbol{I_c = I_c^{ref}\left(\frac{Q_c}{Q_c^{ref}}\right)^{M_c}}, \quad \forall \quad \boldsymbol{c \in \mathscr{C}} \tag{A1}$$

All components (except the heat pump; see chapter 3.1.1) use a fixed component-specific efficiency value that is not influenced by part-load behavior. Degradation is neglected, meaning that efficiencies remain

constant over time. As described in Eq. (A2), the input power ($\dot{Q}_c^{in}$) is a function of the outgoing power ($\dot{Q}_c^{out}$) and the efficiency (η_c) for each component c.

$$\dot{Q}_c^{in} = \frac{\dot{Q}_c^{out}}{\eta_c} \quad , \quad \forall \quad c \in \mathscr{C} \tag{A2}$$

As described in Eq. (A3) for each storage ($s \in \mathscr{S}$), the state of charge definition for the following timestep ($SOC_{s,t+1,}$) consists of the state of charge definition of the current timestep ($SOC_{s,t}$), the charge ($\dot{Q}_{s,t}^{in}$) and discharge power ($\dot{Q}_{s,t}^{out}$) multiplied by the corresponding charge (η_s^{charge}) and discharge ($\eta_s^{discharge}$) efficiencies, the self-discharge of the storage (η_s^{self}) and the respective timestep length (Δt).

$$SOC_{s,\ t+1,} = SOC_{s,\ t}\left(1-\eta_s^{self}\Delta t\right) + \Delta t\left(\dot{Q}_{s,t}^{in}\,\eta_s^{charge} - \frac{\dot{Q}_{s,t}^{out}}{\eta_s^{discharge}}\right), \quad \forall \quad s \in \mathscr{S}, \quad \forall \quad t \in \mathscr{T} \tag{A3}$$

According to Eq. (A4), the state of charge is limited by a relative maximum state of charge ($SOC_s^{\max}$) and a minimum state of charge ($SOC_s^{\min}$), based on the storage capacity (Q_s).

$$SOC_s^{min}\,Q_s \le SOC_{s,t} \le SOC_s^{max}Q_s, \quad \forall \quad s \in \mathscr{S}, \quad \forall \quad t \in \mathscr{T} \tag{A4}$$

Eq. (A5) shows, that for all storages, the state of charge at the start of the time ($SOC_{s,t1}$) has to be on the same level as at the end of the time period ($SOC_{s,tn+1}$).

$$SOC_{s,\ t1,} = SOC_{s,\ tn+1}, \quad \forall \quad s \in \mathscr{S}, \quad \forall \quad t \in \mathscr{T} \tag{A5}$$

The relative minimum ($\alpha_c^{\min}$) and maximum ($\alpha_c^{\max}$) loads of the components output, dependent on the component size (Q_c) when turned on ($x_{c,t} = 1$; off: $x_{c,t} = 0$) is described in Eq. (A6).

$$\alpha_c^{min}\,Q_c x_{c,t} \le \dot{Q}_{c,t}^{out} \le \alpha_c^{max}Q_c x_{c,t}, \quad \forall \quad c \in \mathscr{C}, \quad \forall \quad t \in \mathscr{T} \tag{A6}$$

Table A1
Techno-economic parameters

Component	Parameter	Base	Med	High	Reference
Heat pump	CAPEX [€/kW]	1513	1451[a]	1,325[a]	(Bornemann et al., 2025)
	Reference size [kW]	1			(Bornemann et al., 2025)
	Scale factor [-]	0.7744			(Bornemann et al., 2025)
	Lifetime [a]	25			(Bornemann et al., 2025)
	Maintenance factor [%/a]	1			(Bornemann et al., 2025)
	Min. load [-]	0.2			(Bornemann et al., 2025)
	Max. load [-]	1.0			(Bornemann et al., 2025)
PEM electrolyzer	CAPEX [€/kW]	3750	2988[b]	1,667[b]	(Li et al., 2023)
	Reference size [kW]	1			(Li et al., 2023)
	Scale factor [-]	0.9			(Bornemann et al., 2025)
	Lifetime [a]	15			(Petkov and Gabrielli, 2020)
	Maintenance factor [%/a]	3.5			(Petkov and Gabrielli, 2020)
	Electrical efficiency [-]	0.61	0.66	0.72	(Petkov and Gabrielli, 2020; Potsdam Institute for Climate Impact Research (PIK), 2025)
	Thermal efficiency [-]	0.21			(Bornemann et al., 2025)
	Min. load [-]	0.1			(Bornemann et al., 2025)
	Max. load [-]	1.0			(Bornemann et al., 2025)
PEM fuel cell	CAPEX [€/kW]	3044	2430[c]	1,355[b]	(Li et al., 2023)
	Reference size [kW]	1			(Li et al., 2023)
	Scale factor [-]	0.6889			(Bornemann et al., 2025)
	Lifetime [a]	14			(Petkov and Gabrielli, 2020)
	Maintenance factor [%/a]	3.8			(Petkov and Gabrielli, 2020)
	Electrical efficiency [-]	0.5	0.56	0.62[d]	(Cigolotti et al., 2021; Petkov and Gabrielli, 2020)
	Thermal efficiency [-]	0.3			(Petkov and Gabrielli, 2020)
	Min. load [-]	0.1			(Bornemann et al., 2025)
	Max. load [-]	1.0			(Bornemann et al., 2025)
PV system	CAPEX [€/kW]	1500	1351[d]	856[e]	(Kost et al., 2024)
	Reference size [kW]	1			(Kost et al., 2024)
	Scale factor [-]	0.7914			(Bornemann et al., 2025)
	Lifetime [a]	30			(Kost et al., 2024)
	Maintenance factor [%/a]	1.7			(Petkov and Gabrielli, 2020)
Battery	CAPEX [€/kWh]	750	649[e]	392[f]	(Kost et al., 2024)
	Reference size [kW]	1			(Kost et al., 2024)
	Scale factor [-]	0.8382			(Bornemann et al., 2025)
	Lifetime [a]	15			(Kost et al., 2024)
	Maintenance factor [%/a]	2.2			(Petkov and Gabrielli, 2020)
	Charge / discharge efficiency [-]	0.9			(Kost et al., 2024)
	Charge / discharge max. [kW/kWh]	0.36			(Baumgärtner et al., 2020)

(continued on next page)

Table A1 (*continued*)

Component	Parameter	Base	Med	High	Reference
	Self-discharge [kW/kWh]	$4.2{\cdot}10^{-5}$			(Baumgärtner et al., 2020)
	Min. state of charge [-]	0			(Bornemann et al., 2025)
	Max. state of charge [-]	1			(Bornemann et al., 2025)
Thermal heat storage	CAPEX [€/kWh]	21.7			(Bornemann et al., 2025)
	Reference size [kW]	1			(Bornemann et al., 2025)
	Scale factor [-]	0.8894			(Bornemann et al., 2025)
	Lifetime [a]	24			(Petkov and Gabrielli, 2020)
	Maintenance factor [%/a]	1.5			(Petkov and Gabrielli, 2020)
	Charge / discharge efficiency [-]	0.95			(Sass et al., 2020)
	Charge / discharge max. [kW/kWh]	1.0			(Baumgärtner et al., 2020)
	Self-discharge [kW/kWh]	$5.0{\cdot}10^{-3}$			(Sass et al., 2020)
	Min. state of charge [-]	0			(Bornemann et al., 2025)
	Max. state of charge [-]	1			(Bornemann et al., 2025)
Metal hydride storage	CAPEX [€/kWh]	218	175[g]	119[g]	(Danebergs and Deledda, 2024)
	Reference size [kW]	1			(Danebergs and Deledda, 2024)
	Scale factor [-]	0.7509			(Testi et al., 2023)
	Lifetime [a]	30			(Danebergs and Deledda, 2024)
	Maintenance factor [%/a]	2.0			(Danebergs and Deledda, 2024)
	Reaction enthalpy FeTi [kJ/mol]	-24.6			(Shang et al., 2022)
	Charge / discharge efficiency [-]	1			Assumption
	Charge max. [kW/kWh]	0.75			(Krastev et al., 2023)
	Discharge max. [kW/kWh]	0.38			Assumption based on (Krastev et al., 2023; Wang and Brinkerhoff, 2021)
	Self-discharge [kW/kWh]	0			Assumption
	Efficiency heat exchanger [-]	0.8			(Kumar et al., 2022)
	Min. state of charge [-]	0.1			(Valverde et al., 2016)
	Max. state of charge [-]	0.9			(Valverde et al., 2016)

[a] Learning rate according to (ewi Energy Research & Scenarios gGmbH, 2017).
[b] Learning rate according to (Potsdam Institute for Climate Impact Research (PIK), 2025).
[c] Learning rate according to (Cigolotti et al., 2021).
[d] Expected learning rate according to (Aerospace Technology Institute, 2022).
[e] Linear interpolation according to (Kost et al., 2024).
[f] Extrapolation according to (Kost et al., 2024).
[g] Learning rate according to (Abdin et al., 2022).

Electricity cost data

Table A2
Electricity price data

Parameter	Base	Med	High	References
Electricity price [€/kwh]	0.4022	0.4022	0.4022	(BDEW Bundesverband der Energie- und Wasserwirtschaft e.V., 2025; Prognos AG et al., 2021)
Feed-in-tariff [€/kWh]	0.076	0.04	0.01	(Bundesnetzagentur, 2025; Enercity, 2025)

Software information

The model is Python-based and was implemented in the Pyomo optimization framework (Bynum et al., 2021; Hart et al., 2011). The Gurobi (version 11.0.3) solver was used (Gurobi Optimization, 2025). The relative gap to the optimal solution was set at 5%. The optimization problem is a mixed-integer linear problem (MILP).

Data availability

Data will be made available on request.

References

Abdin, Z., Khalilpour, K., Catchpole, K., 2022. Projecting the levelized cost of large scale hydrogen storage for stationary applications. Energy Convers. Manag. 270, 116241. https://doi.org/10.1016/j.enconman.2022.116241.

Abdolmaleki, L., Jahanbin, A., Berardi, U., 2024. Towards standalone commercial buildings in the Mediterranean climate using a hybrid metal hydride and battery energy storage system. J. Build. Eng. 96, 110567. https://doi.org/10.1016/j.jobe.2024.110567.

ADAC, 2024. Warmwasserspeicher fürs Haus: Welche es gibt und was sie kosten [WWW Document]. URL ⟨https://www.adac.de/rund-ums-haus/energie/versorgung/warmwasserspeicher-fuers-haus/⟩ (accessed 6.3.25).

Aerospace Technology Institute, 2022. Fuel Cells - Roadmap Report.

Baumgärtner, N., Shu, D., Bahl, B., Hennen, M., Hollermann, D.E., Bardow, A., 2020. DeLoop: decomposition-based long-term operational optimization of energy systems with time-coupling constraints. Energy 198, 117272. https://doi.org/10.1016/j.energy.2020.117272.

BDEW Bundesverband der Energie- und Wasserwirtschaft e.V., 2025. BDEW-Strompreisanalyse Mai 2025 [WWW Document]. URL ⟨https://www.bdew.de/service/daten-und-grafiken/bdew-strompreisanalyse/⟩ (accessed 6.4.25).

Bitterer, R., 1999. Repräsentative VDEW- Lastprofile. BTU Cottbus, Lehrstuhl Energiewirtschaft, Prof. Dr. habil. B. Schieferdecker.

Blatter, M., Borel, M., Hediger, H., Simmler, P., 1993. Warmwasserbedarfszahlen und Verbrauchscharakteristik. Bundesamt für Konjunkturfragen, Bern.

Bornemann, L., Lange, J., Kaltschmitt, M., 2025. A rigorous optimization method for long-term multi-stage investment planning: integration of hydrogen into a decentralized multi-energy system. Energy Rep. 13, 117–139. https://doi.org/10.1016/j.egyr.2024.11.079.

Bundesnetzagentur, 2025. Bundesnetzagentur - Archivierte EEG-Vergütungssätze [WWW Document]. URL ⟨https://www.bundesnetzagentur.de/DE/Fachthemen/Elektr

izitaetundGas/ErneuerbareEnergien/EEG_Foerderung/Archiv_VergSaetze/start.html⟩ (accessed 6.4.25).
Bynum, M.L., Hackebeil, G.A., Hart, W.E., Laird, C.D., Nicholson, B.L., Siirola, J.D., Watson, J.-P., Woodruff, D.L., 2021. Pyomo — Optimization Modeling in Python, Springer Optimization and Its Applications. Springer International Publishing, Cham. ⟨https://doi.org/10.1007/978-3-030-68928-5⟩.
Calließ, S., 2024. Wie hoch ist der Energieverbrauch im Haus einer Durchschnittsfamilie? [WWW Document]. Wie hoch ist der Energieverbrauch der Durchschnittsfamilie? URL ⟨https://www.thermondo.de/info/rat/heizen/energieverbrauch-durchschnittsfamilie/⟩ (accessed 5.15.25).
Cigolotti, V., Genovese, M., Fragiacomo, P., 2021. Comprehensive review on fuel cell technology for stationary applications as sustainable and efficient poly-generation energy systems. Energies 14, 4963. https://doi.org/10.3390/en14164963.
Ciocia, A., Amato, A., Di Leo, P., Fichera, S., Malgaroli, G., Spertino, F., Tzanova, S., 2021. Self-consumption and self-sufficiency in photovoltaic systems: effect of grid limitation and storage installation. Energies 14, 1591. https://doi.org/10.3390/en14061591.
Danebergs, J., Deledda, S., 2024. Can hydrogen storage in metal hydrides be economically competitive with compressed and liquid hydrogen storage? A techno-economical perspective for the maritime sector. Int. J. Hydrogen Energy 50, 1040–1054. https://doi.org/10.1016/j.ijhydene.2023.08.313.
Drawer, C., Lange, J., Kaltschmitt, M., 2024. Metal hydrides for hydrogen storage – Identification and evaluation of stationary and transportation applications. J. Energy Storage 77, 109988. https://doi.org/10.1016/j.est.2023.109988.
Durán Gómez, P., Echevarría Camarero, F., Ogando-Martínez, A., Carrasco Ortega, P., 2023. Profitability of alternative battery operation strategies in photovoltaic self-consumption systems under current regulatory framework and electricity prices in Spain. Energies 16, 7375. https://doi.org/10.3390/en16217375.
DVGW, 2004. DVGW W 551 - 2004-04 - DIN Media [WWW Document]. URL ⟨https://www.dinmedia.de/en/technical-rule/dvgw-w-551/74193855⟩ (accessed 6.4.25).
Enercity, 2025. Photovoltaik-Einspeisevergütung 2024 und 2025 [WWW Document]. URL ⟨https://www.enercity.de/magazin/mein-leben/photovoltaik-einspeisevergetung⟩ (accessed 6.4.25).
ewi Energy Research & Scenarios gGmbH, 2017. Energiemarkt 2030 und 2050 – Der Beitrag von Gas- und Wärmeinfrastruktur zu einer effizienten CO2-Minderung.
Gasag, 2024. Stromverbrauch im Einfamilienhaus [WWW Document]. URL ⟨https://www.gasag.de/magazin/energiesparen/stromverbrauch-einfamilienhaus/⟩ (accessed 4.1.25).
Gonschor, A., 2024. Wärmepumpe dimensionieren – so finden Sie die richtige Größe. Wegatech powered by heimWatt. URL ⟨https://www.wegatech.de/ratgeber/waermepumpe/planung-und-installation/dimensionierung/⟩ (accessed 6.3.25).
Gudmunds, D., Nyholm, E., Taljegard, M., Odenberger, M., 2020. Self-consumption and self-sufficiency for household solar producers when introducing an electric vehicle. Renew. Energy 148, 1200–1215. https://doi.org/10.1016/j.renene.2019.10.030.
Gurobi Optimization, 2025. Gurobi optimizer reference manual [WWW Document]. URL ⟨https://www.gurobi.com/⟩.
Hart, W.E., Watson, J.-P., Woodruff, D.L., 2011. Pyomo: modeling and solving mathematical programs in Python. Math. Prog. Comp. 3, 219–260. https://doi.org/10.1007/s12532-011-0026-8.
Kebede, A.A., Kalogiannis, T., Van Mierlo, J., Berecibar, M., 2022. A comprehensive review of stationary energy storage devices for large scale renewable energy sources grid integration. Renew. Sustain. Energy Rev. 159, 112213. https://doi.org/10.1016/j.rser.2022.112213.
Klopčič, N., Grimmer, I., Winkler, F., Sartory, M., Trattner, A., 2023. A review on metal hydride materials for hydrogen storage. J. Energy Storage 72, 108456. https://doi.org/10.1016/j.est.2023.108456.
Kost, C., Müller, P., Schweiger, J.S., Fluri, V., Thomson, J., 2024. Levelized Cost of Electricity - Renewable Energy Technologies.
Krastev, V., Bella, G., Falcucci, G., Bartolucci, L., Cordiner, S., Mulone, V., 2023. Power Vs. Capacity Performances of Thermally Integrated MH-PCM Hydrogen Storage Solutions: Current Status and Development Perspectives. 36th International Conference on Efficiency, Cost, Optimization, Simulation and Environmental Impact of Energy Systems (ECOS 2023). Presented at the 36th International Conference on Efficiency, Cost, Optimization, Simulation and Environmental Impact of Energy Systems (ECOS 2023). ECOS 2023, Las Palmas De Gran Canaria, Spain, pp. 2183–2193. https://doi.org/10.52202/069564-0197.
Krützfeldt, H., Vering, C., Mehrfeld, P., Müller, D., 2021. MILP design optimization of heat pump systems in German residential buildings. Energy Build. 249, 111204. https://doi.org/10.1016/j.enbuild.2021.111204.
Kumar, K., Alam, M., Dutta, V., 2019. Techno-economic analysis of metal hydride-based energy storage system in microgrid. Energy Storage 1, e62. https://doi.org/10.1002/est2.62.
Kumar, S., Sharma, R., Srinivasa Murthy, S., Dutta, P., He, W., Wang, J., 2022. Thermal analysis and optimization of stand-alone microgrids with metal hydride based hydrogen storage. Sustain. Energy Technol. Assess. 52, 102043. https://doi.org/10.1016/j.seta.2022.102043.
Kümpel, N., 2024. PV-Anlage Größe berechnen – so gelingt die Dimensionierung. Wegatech powered by heimWatt. URL ⟨https://www.wegatech.de/ratgeber/photovoltaik/planung-und-installation/dimensionierung-pv-anlage/⟩ (accessed 6.3.25).
Li, N., Lukszo, Z., Schmitz, J., 2023. An approach for sizing a PV–battery–electrolyzer–fuel cell energy system: a case study at a field lab. Renew. Sustain. Energy Rev. 181, 113308. https://doi.org/10.1016/j.rser.2023.113308.
Liebensteiner, M., Ocker, F., Abuzayed, A., 2025. High electricity price despite expansion in renewables: how market trends shape Germany's power market in the coming years. Energy Policy 198, 114448. https://doi.org/10.1016/j.enpol.2024.114448.
Mehr, A.S., Phillips, A.D., Brandon, M.P., Pryce, M.T., Carton, J.G., 2024. Recent challenges and development of technical and technoeconomic aspects for hydrogen storage, insights at different scales; a state of art review. Int. J. Hydrogen Energy 70, 786–815. https://doi.org/10.1016/j.ijhydene.2024.05.182.
Meriläinen, A., Montonen, J.-H., Kosonen, A., Lindh, T., Ahola, J., 2023. Cost-optimal dimensioning and operation of a solar PV–BESS–heat pump-based on-grid energy system for a Nordic climate townhouse. Energy Build. 295, 113328. https://doi.org/10.1016/j.enbuild.2023.113328.
Möller, M.C., Krauter, S., 2022. Hybrid energy system model in matlab/simulink based on solar energy, lithium-ion battery and hydrogen. Energies 15, 2201. https://doi.org/10.3390/en15062201.
Muñoz Robinson, C., Reininghaus, N., Pistoor, A., Kröner, M., Dyck, A., Vehse, M., Lange, J., Kaltschmitt, M., Puszkiel, J., Covarrubias, M., Fleming, L., Kaufmann, T., Krause, P., Warfsmann, J.H., Wienken, E.S., Wildner, L., Klassen, T., Jepsen, J., 2024. Dispatch optimization of the electricity and heat of the smart-energy-transform-unit. https://doi.org/10.24405/16775.
Nivedhitha, K.S., Beena, T., Banapurmath, N.R., Umarfarooq, M.A., Ramasamy, V., Soudagar, M.E.M., Ağbulut, Ü., 2024. Advances in hydrogen storage with metal hydrides: mechanisms, materials, and challenges. Int. J. Hydrogen Energy 61, 1259–1273. https://doi.org/10.1016/j.ijhydene.2024.02.335.
Observ'ER., TNO, Renewables Academy (RENAC) AG, Fraunhofer ISI, VITO (Flemish Institute for Technological Research), Statistics Netherlands, 2024. The state of renewable energies in Europe - 2024 (No. 23rd EurObserv'ER Report).
Olympios, A.V., Justo Alonso, M., Pantaleo, A.M., 2025. Heat pumps in Europe: perspectives and innovation challenges. Prog. Energy 7, 032004. https://doi.org/10.1088/2516-1083/ade94a.
Orth, N., Weniger, J., Meissner, L., 2022. Empfehlungen zur Auslegung von Solarstromspeichern. HTW Berlin. URL ⟨https://solar.htw-berlin.de/publikationen/auslegung-von-solarstromspeichern/⟩ (accessed 6.3.25).
Petkov, I., Gabrielli, P., 2020. Power-to-hydrogen as seasonal energy storage: an uncertainty analysis for optimal design of low-carbon multi-energy systems. Appl. Energy 274, 115197. https://doi.org/10.1016/j.apenergy.2020.115197.
Potsdam Institute for Climate Impact Research (P.I.K.), 2025. Price of Hydrogen: CAPEX Data [WWW Document]. URL ⟨https://h2.pik-potsdam.de/H2Dash/#section-visualisations⟩ (accessed 5.22.25).
Prognos A.G., Fraunhofer I.S.I., G.W.S., IINAS, 2021. Energiewirtschaftliche Projektionen und Folgeabschätzungen 2030/2050.
Recent Facts about Photovoltaics in Germany, Harry Wirth, Fraunhofer ISE, Download from https://www.pv-fakten.de/, Version update 18.08.2025.
Renewables.ninja, 2025. Renewables.ninja [WWW Document]. URL ⟨https://www.renewables.ninja/⟩ (accessed 6.4.25).
Rieck, K., Dabrock, K., Pflugradt, N., Weinand, J.M., Stolten, D., 2025. Large-scale quantification of the future self-covered heat demand using a nationwide residential building database. Energy 317, 134622. https://doi.org/10.1016/j.energy.2025.134622.
Rivarolo, M., Raggio, M., Montagna, G.N., Barberis, S., 2024. Feasibility study and optimal sizing of H2 storage and PEM fuel cells onboard ships. J. Phys. Conf. Ser. 2893, 012075. https://doi.org/10.1088/1742-6596/2893/1/012075.
Rövekamp, P., Schöpf, M., Wagon, F., Weibelzahl, M., Fridgen, G., 2021. Renewable electricity business models in a post feed-in tariff era. Energy 216, 119228. https://doi.org/10.1016/j.energy.2020.119228.
Sass, S., Faulwasser, T., Hollermann, D.E., Kappatou, C.D., Sauer, D., Schütz, T., Shu, D. Y., Bardow, A., Gröll, L., Hagenmeyer, V., Müller, D., Mitsos, A., 2020. Model compendium, data, and optimization benchmarks for sector-coupled energy systems. Comput. Chem. Eng. 135, 106760. https://doi.org/10.1016/j.compchemeng.2020.106760.
Sens, L., Piguel, Y., Neuling, U., Timmerberg, S., Wilbrand, K., Kaltschmitt, M., 2022. Cost minimized hydrogen from solar and wind – production and supply in the European catchment area. Energy Convers. Manag. 265, 115742. https://doi.org/10.1016/j.enconman.2022.115742.
Shang, Y., Liu, S., Liang, Z., Pyczak, F., Lei, Z., Heidenreich, T., Schökel, A., Kai, J., Gizer, G., Dornheim, M., Klassen, T., Pistidda, C., 2022. Developing sustainable FeTi alloys for hydrogen storage by recycling. Commun. Mater. 3. https://doi.org/10.1038/s43246-022-00324-5.
Spalthoff, C., Ulffers, J., Prade, E., Kneiske, T., Lenz, M., Braun, M., 2022. FLEXIBLE WÄRMEPUMPEN IM VERTEILNETZ.
Testi, M., Prattico, L., Ragaglia, D., 2023. HyCARE Hydrogen CArrier for Renewable Energy Storage - Techno-economic analysis.
Umweltbundesamt, 2023. Richtiges Heizen schützt das Klima und den Geldbeutel [WWW Document]. URL ⟨https://www.umweltbundesamt.de/umwelttipps-fuer-den-alltag/heizen-bauen/heizen-raumtemperatur⟩ (accessed 5.15.25).
Valverde, L., Bordons, C., Rosa, F., 2016. Integration of fuel cell technologies in renewable-energy-based microgrids optimizing operational costs and durability. IEEE Trans. Ind. Electron. 63, 167–177. https://doi.org/10.1109/TIE.2015.2465355.
VDI, 2007. Meteorologische Daten in der technischen Gebäudeausrüstung Gradtage.
Wang, C.-S., Brinkerhoff, J., 2021. Predicting hydrogen adsorption and desorption rates in cylindrical metal hydride beds: Empirical correlations and machine learning. Int. J. Hydrogen Energy 46, 24256–24270. https://doi.org/10.1016/j.ijhydene.2021.05.007.
Wang, X., Peng, P., Witman, M.D., Stavila, V., Allendorf, M.D., Breunig, H.M., 2025. Technoeconomic insights into metal hydrides for stationary hydrogen storage. Adv. Sci. 12, 2415736. https://doi.org/10.1002/advs.202415736.
Willuhn, M., 2024. Österreich und Schweiz: HPS erweitert Vertrieb seines Wasserstoffspeichers ins Ausland [WWW Document]. pv magazine Deutschland.

URL ⟨https://www.pv-magazine.de/2024/11/06/oesterreich-und-schweiz-hps-erweitert-vertrieb-von-wasserstoffspeicher-ins-ausland/⟩ (accessed 6.3.25).

Wüllhorst, F., Reuter-Schniete, J., Maier, L., Müller, D., 2024. Heat pump and thermal energy storage: Influences of photovoltaic, the control strategy, and price assumptions on the optimal design. Renew. Energy 236, 121409. https://doi.org/10.1016/j.renene.2024.121409.

Ye, H., Chen, F., Pei, Y., Hou, Z., Zhang, B., Hu, H., 2025. High-efficiency thermal management solutions for metal hydride-based residential hydrogen storage systems. Energy Convers. Manag. 344, 120337. https://doi.org/10.1016/j.enconman.2025.120337.